AD-A128 785 DOPPLER PROCESSING OF RADAR CLUTTER ECHOES WITH LIMITED RANGE EXTENTS(U) NAVAL RESEARCH LAB WASHINGTON DC B H CANTRELL 27 MAY 83 NRL-8693 1/1

UNCLASSIFIED F/G 17/9 NL

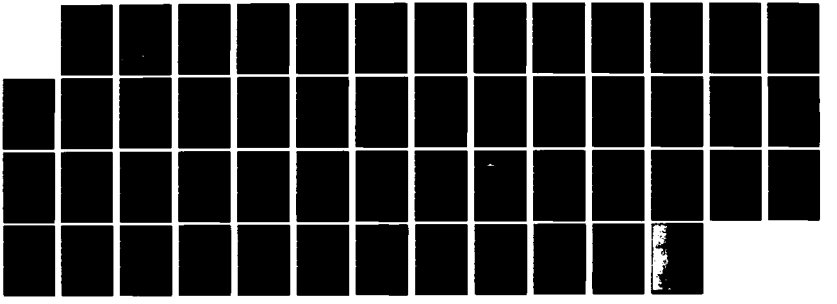

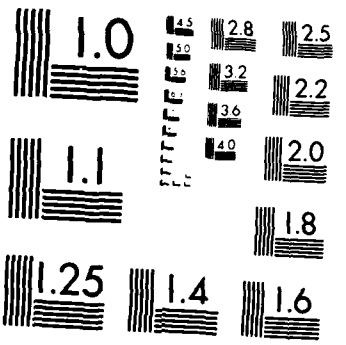

NRL Report 8693

Doppler Processing of Radar Clutter Echoes with Limited Range Extents

BEN CANTRELL

Radar Analysis Branch
Radar Division

May 27, 1983

NAVAL RESEARCH LABORATORY
Washington, D.C.

SECURITY CLASSIFICATION OF THIS PAGE (When Data Entered)

REPORT DOCUMENTATION PAGE	READ INSTRUCTIONS BEFORE COMPLETING FORM
1 REPORT NUMBER NRL Report 8693	2 GOVT ACCESSION NO AD-A128785
3 RECIPIENT'S CATALOG NUMBER	
4 TITLE (and Subtitle) DOPPLER PROCESSING OF RADAR CLUTTER ECHOES WITH LIMITED RANGE EXTENTS	5 TYPE OF REPORT & PERIOD COVERED Interim report on a continuing NRL problem.
	6 PERFORMING ORG REPORT NUMBER
7 AUTHOR(s) B.H. Cantrell	8 CONTRACT OR GRANT NUMBER(s)
9 PERFORMING ORGANIZATION NAME AND ADDRESS Naval Research Laboratory Washington, DC 20375	10 PROGRAM ELEMENT, PROJECT, TASK AREA & WORK UNIT NUMBERS 61153N RR-021-05-41 NRL Problem 53-0628-00
11 CONTROLLING OFFICE NAME AND ADDRESS Office of Naval Research Arlington, VA 22217	12 REPORT DATE May 27, 1983
	13 NUMBER OF PAGES 50
14 MONITORING AGENCY NAME & ADDRESS(if different from Controlling Office)	15 SECURITY CLASS. (of this report) UNCLASSIFIED
	15a DECLASSIFICATION/DOWNGRADING SCHEDULE

16 DISTRIBUTION STATEMENT (of this Report)

Approved for public release; distribution unlimited.

17 DISTRIBUTION STATEMENT (of the abstract entered in Block 20, if different from Report)

18 SUPPLEMENTARY NOTES

19 KEY WORDS (Continue on reverse side if necessary and identify by block number)

MTI
Pulse Doppler
Radar signal processing
Clutter cancelers

20 ABSTRACT (Continue on reverse side if necessary and identify by block number)

The Doppler processing of radar echoes from clutter patches of finite range extent was studied. The results of the study show that if the range extent of the clutter patches is known or measured, and if the parameters of the radar's pulse bursts and Doppler processor are set based on this knowledge, then performance can be significantly improved under many cases.

DD FORM 1 JAN 73 1473 EDITION OF 1 NOV 65 IS OBSOLETE
S/N 0102-014-6601

SECURITY CLASSIFICATION OF THIS PAGE (When Data Entered)

CONTENTS

EXECUTIVE SUMMARY iv

INTRODUCTION 1

REPRESENTATIONS 2

- Transmitted Signal 2
- Received Signal 3
- Transversal Filters 8
- Time Alignment 9
- Target Detector 12

BASIC THEOREMS AND DEFINITIONS 14

- Orthogonality Conditions 15
- Rearrangement Theorem 15
- Separation Time Intervals 16
- Time-Alignment Theorem 19
- Segmented Clutter Signals 19
- Eclipsing Conditions 21

PULSE-DOPPLER AND MTI OPERATION 23

- Pulse-Doppler and MTI Definitions 23
- Requirement on Transmitted Pulses 25
- Pulse-Doppler Clutter Stacking Theorem 25
- A Counting Theorem 25
- Range Ambiguities 26

CONTROLLED-PULSE-DOPPLER OPERATION 26

- Definition of Controlled-Pulse-Doppler Operation 26
- Requirement on Transmitted Pulses 27
- Controlled-Pulse-Doppler Clutter Stacking Theorem 27
- A Counting Theorem 27
- Separation Requirements 27
- Range Ambiguities 30
- Example of Performance 30

SUMMARY 32

REFERENCES 33

APPENDIX A — Proofs of Basic Theorems 34

APPENDIX B — Proofs on Pulse-Doppler and MTI Operation 40

APPENDIX C — Proofs on Controlled Pulse Doppler (CPD) Operation 45

EXECUTIVE SUMMARY

Radars are now designed to distinguish moving targets from stationary background by Doppler processing of the pulse echoes. In practice, sometimes it is difficult for radars to separate some kinds of clutter patches from targets. This report describes how a radar can be designed to operate such that the clutter and targets can be separated.

A Doppler processing process is described which accounts for the range extent of clutter patches that can be measured. A pulse burst (N pulses separated by a fixed interval of time) is transmitted, and the echoes are received until the echoes are so weak that none are detectable. The radar echoes are passed through a conventional Doppler processor. The Doppler processing must be matched to the range extent of the clutter in the following manner. Loosely, the range extent of the pulse burst must exceed the range extent of the clutter patch for the Doppler-processing filter to reach steady-state conditions so that a target and the clutter can be separated. Furthermore, to keep transient signals due to one clutter patch from corrupting the steady-state signals from another clutter patch, the order of the filter times the pulse spacing must be less than the range extent of the separation between the clutter patches. If these two conditions can be met, it is possible to separate targets from various clutter patches independently with short pulse bursts. This process is called controlled-pulse-Doppler (CPD) operation.

The advantages of CPD operation are that short times between pulses can be obtained so as to yield excellent cancellation, no clutter stacking is found from patch to patch, range ambiguities need to be resolved only within a clutter patch rather than at all ranges, and there is little to no eclipsing. Consequently, if the clutter is patchy and/or limited in range extent, significant improvements can be obtained in radar Doppler processing by matching it to the measured environment. The subsequent development is quite mathematical and is meant to place the processes on a firm mathematical foundation. It most likely will be difficult reading. It is written for those that are concerned with detailed design of radars.

DOPPLER PROCESSING OF RADAR ECHOES WITH LIMITED RANGE EXTENTS

INTRODUCTION

In this report a study will be presented of the Doppler processing of radar echoes from clutter patches of finite range extent. This study shows how radar performance can be significantly improved in many cases. So that the presentation of this study can be properly understood, however, much of the content of this report will be prologue.

Radar systems are used to detect and locate distant objects through the use of electromagnetic reflections. These systems work by emitting radiation, and upon reception of the reflected energy from the object the angle of arrival of the signal entering the antenna is determined and the range is determined by the time delay in the modulated transmitted signal. In addition, the echo signal is Doppler shifted by the radial speed of the reflector. It is the processing of the transmitted signal which has been reflected and Doppler shifted by the target which is the concern of this report.

The earliest radar systems in the 1920s and early 1930s used the Doppler shift in continuous-wave (CW) radars to provide the mechanism for detection. After the development of the duplexer in the mid 1930s, the emphasis was shifted to pulsed monostatic radars [1]. During World War II the Doppler information on the pulse was used to discriminate the moving targets from the fixed targets. This was first accomplished by operators observing the amplitude fluctuations from pulse to pulse on the A-scope which were caused by the target beating with clutter at the range of a target. Development of coherent moving-target-indicator (MTI) systems was also initiated during World War II. This system could recognize the moving targets from the fixed targets even when clutter was not present [2]. After World War II the development of radar systems which used coherent Doppler processing became common, and since 20 to 30 years ago many radar systems have used Doppler processing. These systems include long-range-surveillance, fire-control, over-the-horizon (OTH), point-defense, synthetic-aperture (SAR), and airborne-surveillance radars. Not only has considerable hardware been fielded over the years, but considerable theory exists in the literature. Standard handbooks such as Refs. 1, 3, 4, and 5 can be referred to for further information. It is hopeless to review this enormous body of literature in this report. Instead I will outline the situation I wish to address in context with current standard practices.

In pulsed coherent radar systems the Doppler processing is accomplished by passing the echoes from a group of identical radiated microwave pulses through linear filters. Two of these systems are classically named the MTI system and the pulse-Doppler system. The MTI system uses interpulse spacing (pulse-repetition interval) long enough that no range ambiguities exist. The pulse-Doppler system uses interpulse spacing short enough that no velocity ambiguity exists.* Often in practice neither of these conditions are achieved. The problem which occurs in most systems can be described as follows. In systems with long pulse-repetition intervals some kinds of wind-blown clutter decorrelate from pulse to pulse, nullifying the benefits of the filtering. When the pulse-repetition interval is decreased to achieve more correlation in the clutter from pulse to pulse, the following effects are observed: range ambiguities are introduced, sometimes clutter stacking from more than one range is obtained, and better clutter cancellation is required because weak far-range targets compete with strong close-in

Manuscript approved January 20, 1983.

*This operation at a high pulse-repetition frequency is usually referred to as high-PRF pulse Doppler. Medium-PRF pulse Doppler has both range and Doppler ambiguities.

clutter. In all these cases enough pulses must be used such that steady-state conditions are obtained. If the filters are observed during the transient period or before all the pulses required for steady-state conditions are processed, often unrecognizable results are obtained. Simple examples of the transient conditions are described on page 131 of Ref. 1. It is the relation between a group of pulses, called a pulse burst, and the clutter characteristics which we are concerned with in this study.

Clutter has finite range extent and often occurs in patches. Examples are a rain storm, an island, sea clutter near a ship's radar, and a coastline. The clutter patches or clouds are usually characterized by their range extent, range separation from other patches, spectral spread or decorrelation time, and amplitude probability density which specifies the mean and variances of the clutter level. Usually the angle extent of the clutter changes by only a small amount over the processing time of the pulse burst and is not included in the above list of clutter-patch properties. The effect of the small angle changes of the beam is to cause a small decorrelation in the clutter. The operation and performance of Doppler processors with respect to most of the clutter-patch characteristics have been studied extensively. However, little has been done to incorporate the range extent and spacing of multiple clutter patches into the analysis. I am going to present a study of the operation and performance of Doppler processors when the processing includes the range extent and spacing of multiple clutter patches.

I begin setting the stage for presenting the study by describing the signals and the operations on those signals. These I will represent in a mathematical form. I will next give basis definitions and develop the fundamental theorems. Within this mathematical structure I will finish setting the stage by describing conventional pulse-Doppler and MTI operations under special restrictions. In presenting the study, I will remove these restrictions and develop the requirements for proper operation with respect to the range extent and separation of clutter patches. Finally I will describe the performance analytically for some examples, showing that for these examples proper radar operation based on knowledge about the clutter patches significantly improves the performance.

REPRESENTATIONS

I begin setting the stage for presenting the study by defining in detail the signals and processes which are used throughout the report. The basic signal flow and operations are illustrated in Fig. 1. The radar generates a waveform (a group of pulses) $\delta(t)$ and transmits it through an antenna. The reflections along with receiver noise and external interference are received. The received signal is denoted by $X(t)$. With use of conventional coherent radar receivers, the received signal is converted to baseband and matched-filtered. The resulting complex baseband signals are denoted by $X_p(t)$. Conventional Doppler processing is then performed by transversal filters, resulting in signals $Y_p(t, \mathrm{v}, [0])$. A time-alignment operation whose output is $Z_{pq}(t, \mathrm{v})$ is next performed by linear delay lines. Finally a rather conventional constant-false-alarm-rate (CFAR) detection process is performed. The detection time history is denoted by $D(t, \mathrm{v})$. I next define and describe each of the processes and signals $\delta(t)$, $X(t)$, $X_p(t)$, $Y_p(t, \mathrm{v}, [0])$, $Z_{pq}(t, \mathrm{v})$, and $D(t, \mathrm{v})$.

Transmitted Signal

The narrow-bandwidth transmitted signal, centered on the carrier frequency ω_{ij}, is defined in a conventional way by

$$\mathrm{Re}\{\delta(t)e^{+j\omega_{ij}t}\}, \tag{1}$$

where t is time, j is $\sqrt{-1}$, and Re represents the real part of the argument in the braces. Furthermore the baseband complex signal $\delta(t)$ of narrow bandwidth with respect to the carrier is defined by

$$\delta(t) = \sum_{i=1}^{N} \sum_{j=1}^{N_i} \delta_{ij}(t, (\lambda_i + \tau_{ij})), \tag{2}$$

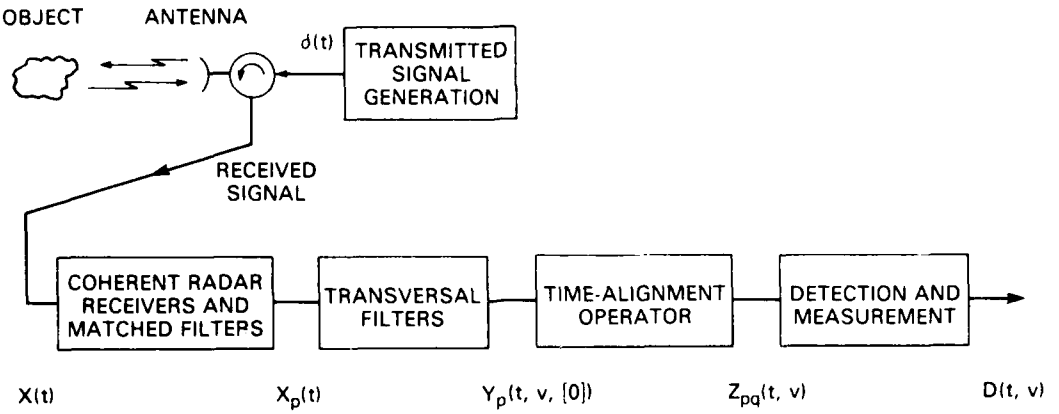

Fig. 1 — Signal flow throughout the complete system

where N is the number of pulse trains, N_i is the number of pulses in the ith pulse train, λ_i is the time delay between the leading edge of first pulse of the $(i = 1)$th pulse train to the leading edge of the first pulse of the ith pulse train, and τ_{ij} is the time delay between the leading edge of the jth pulse of the ith pulse train and the leading edge of the first pulse of the ith pulse train. Furthermore $\delta_{ij}(t, (\lambda_i + \tau_{ij}))$ is a complex signal of finite time duration $\bar{\zeta}_i$ which represents the baseband signal of the jth pulse in the ith pulse train delayed in time by $\lambda_i + \tau_{ij}$. By definition we require $\bar{\zeta}_i < \tau_{ij}$ so that the transmitter is not transmitting two different pulses simultaneously in the same pulse train.

In the remaining development, we require the carrier frequency, the spacing between pulses, and the complex baseband signal be the same for all pulses in the ith pulse train. Consequently we define ω_i and τ_i by

$$\omega_{ij} = \omega_i, \quad \text{for all } j,$$

and

$$\tau_{ij} = (j - 1)\tau_i$$

and note $\delta_{ig}(\cdot) = \delta_{ih}(\cdot)$ for all g and h. Although not necessary, we further require the number of pulses in all the pulse trains to be the same and define $\bar{N}$ such that

$$\bar{N} = N_i, \quad \text{for all } i.$$

The counting of the pulse trains is sequential, so that

$$\lambda_g > \lambda_h, \quad \text{for } g > h.$$

The maximum time interval between pulses is defined by

$$\bar{\tau} = \text{maximum value of } \tau_i \text{ for all } i.$$

We further define $\tau_g > \tau_h$ for $g > h$. Finally we define $\bar{\zeta} = \bar{\zeta}_i$ for all i, which means that all the pulses have the same width $\bar{\zeta}$. The waveform in Fig. 2 illustrates the magnitude of the complex baseband signal $\delta(t)$. The phase portion is not shown.

Received Signals

The received signal is composed of reflected signals, externally generated interference signals, and noise. In the following discussions we will assume that no external interfering source is present. The

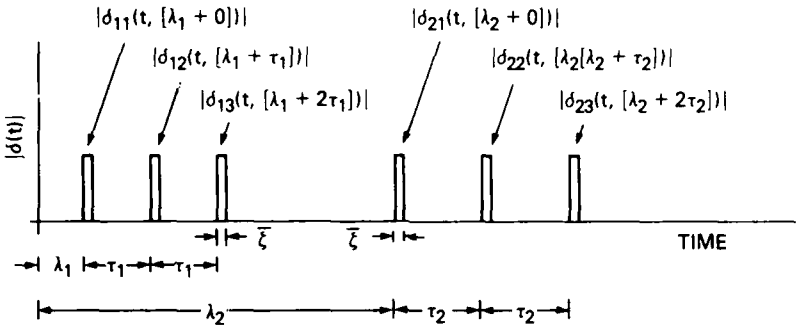

Fig. 2 — Magnitude of the complex baseband transmitted signal $|\delta(t)|$ for $N = 2$ and $\bar{N} = 3$

noise consists of external noise entering the radar added to the radar's front-end noise. The noise is assumed to be white and Gaussian with a time-varying and unknown power level. The radar echoes are divided into two categories, defined as targets and clutter. These categories are rather arbitrary in that targets are considered the desired echoes and clutter the undesired echoes. Targets such as aircraft are usually characterized by echoes of limited range extent and by their motion in time. Other echoes which are often considered clutter such as from land, sea, and rain usually have no or small motions, and the reflections are extended in range.

After the signal is received at the antenna, it is passed through multiple conventional coherent radar receivers and matched filters. The conventional coherent radar receivers usually involve several linear frequency translations, multiple filters to reject out-of-band signals, amplification, and a conversion to baseband. The baseband-signal is a complex signal, with the in-phase component being the real part and the quadrature component being the imaginary part. All frequency translations are integrally related to the carrier frequency ω_i so there is phase coherence between pulses of the ith pulse train. A conventional matched filter (matched to each transmitted pulse) is included in each receiver. We define the pulse width (zero crossing to zero crossing) after matched filtering of a target echo due to a point target to be 2ζ. Consequently if the radar employs pulse compression, the pulse-compression ratio is approximately $\bar{\zeta}/\zeta$. Of course some radars do not use pulse compression, and for those cases $\bar{\zeta}/\zeta \approx 1$. The entire process in the coherent radar receiver and matched filter is linear. We define a linear operator $F_p(\cdot)$ so that the outputs of the receivers can be related to its inputs by

$$X_p(t) = F_p(X(t)),$$

where $X(t)$ is the received signal from the antenna and $X_p(t)$ is the complex baseband signal out of the pth receiver. The signal flow of the receiver structure is shown in Fig. 3. The reason $p = N$ receivers are used is that the pulse trains can occur over the same interval of time and be at different frequencies. Some of the cases to be studied later apply certain constraints which allow fewer or a single receiver. However, for now we allow the process to be described more generally.

We need to describe in detail the received signal at one point along the signal-processing chain. The signals at all other stages along the processing chain can then be represented in terms of the defined signal and the processes performed. We choose to define the received signals $X_p(t)$ in detail. The signals out of subsequent processors are then later defined in terms of the signals representing $X_p(t)$. Although we could also represent the signals after various processes back toward the antenna in terms of the signals $X_p(t)$, we do not, because these signals are not required in the remaining analysis.

The complex baseband signals are written as

$$X_p(t) = C_p(t) + T_p(t) + N_p(t), \tag{3}$$

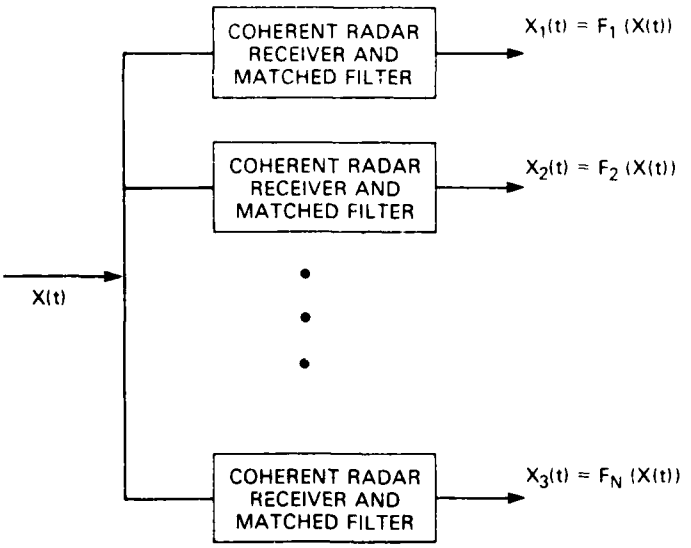

Fig. 3 — Signal flow through conventional coherent radar receivers and matched filters

where the complex baseband signals due to clutter $C_p(t)$ are

$$C_p(t) = \sum_{k=1}^{N_c} \sum_{i=1}^{N} \sum_{j=1}^{\bar{N}} C_{ijp}(t,\ k,\ [\bar{\zeta} + \lambda_i + \tau_{ij}]). \tag{4}$$

The complex baseband signals due to targets $T_p(t)$ are

$$T_p(t) = \sum_{l=1}^{N_t} \sum_{i=1}^{N} \sum_{j=1}^{\bar{N}} T_{ijp}(t,\ l,\ [\bar{\zeta} + \lambda_i + \tau_{ij}]), \tag{5}$$

and the complex baseband signal due to noise is $N_p(t)$, where $p = 1, 2, \ldots, N$. Furthermore, N_c and N_t are the number of clutter patches and targets respectively, and $C_{ijp}(t, k, [\bar{\zeta} + \lambda_i + \tau_{ij}])$ and $T_{ijp}(t, l, [\bar{\zeta} + \lambda_i + \tau_{ij}])$ are the complex baseband signal representations of the radar echoes reflected from the k th clutter patch and l th target respectively due to the j th pulse of the i th pulse train passing through the p th receiver. The circuit time delays are $\bar{\zeta} + \lambda_i + \tau_{ij}$. The total time delays including those associated with the echoes are defined as follows. The time delay associated with the l th target echo is obtained by observing the time delay between the center of the l th target echo due to the j th pulse of the i th pulse train and the leading edge of the first pulse of the first pulse of the transmitted pulse train. This differential time delay is

$$\gamma_l + (\bar{\zeta} + \lambda_i + \tau_{ij}),$$

where γ_l is the time delay associated with the range to the l th target echo, $\lambda_i + \tau_{ij}$ is the delay of the j th pulse in the i th pulse train, and $\bar{\zeta}$ is the delay from the matched filter.

The time delays α_k and β_k, associated with the leading edge and trailing edge of the k th clutter patch respectively, are obtained by observing the time delays between both the leading and trailing edges, defined at the time the signal is first nonzero and at the time it just becomes zero respectively, of the k th clutter patch echo due to the j th pulse of the i th pulse train and the leading edge of the first pulse of the transmitted pulse train. These differential time delays are

$$\alpha_k + (\zeta + \lambda_i + \tau_{ij})$$

and

$$\beta_k + (\bar{\zeta} + \lambda_i + \tau_{ij}),$$

where α_k and β_k are the time delays associated with the range to the leading and trailing edges of the k th clutter patch respectively and $(\bar{\zeta} + \lambda_i + \tau_{ii})$ is the circuit delay due to the transmitted pulse delays and matched filter. The width in time of the kth clutter patch is then given by

$$\beta_k - \alpha_k.$$

The target range extents are assumed to be small relative to the pulse width described in range, so that the target echo width is the pulse width ζ. We further define

$$\gamma_g > \gamma_h$$

and

$$\alpha_g > \alpha_h$$

for $g > h$ so that the echoes are ordered in range.

The complex baseband signals $X_p(t)$ are illustrated in Figs. 4 and 5. In both cases there are $\bar{N} = 3$ pulses in the $N = 2$ pulse trains. The magnitude of the transmitted pulses are shown in both figures, with the resulting magnitudes of the complex baseband signals $X_1(t)$ and $X_2(t)$ due to a single target being shown in Fig. 4 and the resulting magnitudes due to a single clutter patch being shown in Fig. 5. No pulse compression was used. If the frequencies ω_1 and ω_2 were well separated so that the signals from different pulse trains could be easily separated by filters, the dotted portions of the echoes would not be present. Later this condition will be defined as the frequency orthogonality condition. However, if $\omega_1 = \omega_2$, then the dotted portions would be present, and if the targets or clutter did not decorrelate significantly over the time frame, the signal magnitudes of all echoes would appear nearly the same. In these examples echoes from the first and second pulse trains do not overlap in time. This condition will later be defined as the time orthogonality condition. For now we allow the signals to overlap in frequency and time.

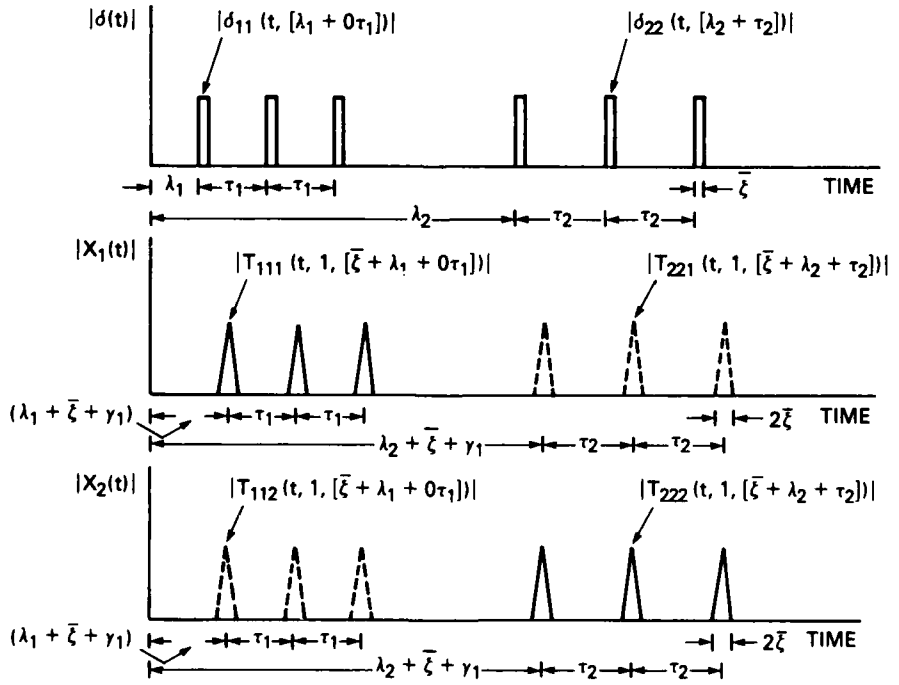

Fig. 4 — Illustration of a target echo after conversion to baseband for $N = 2$, $\bar{N} = 3$, and $\zeta = \bar{\zeta}$

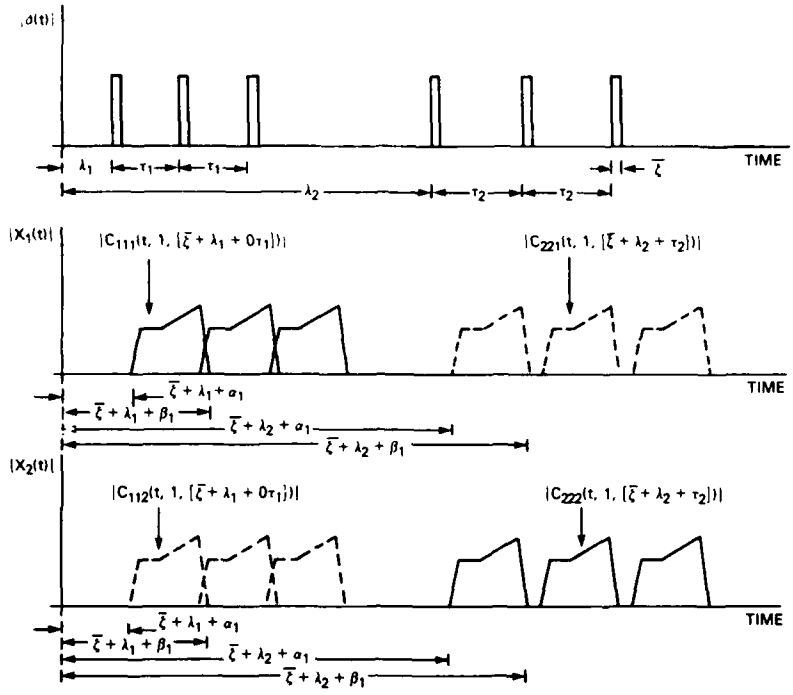

Fig. 5 — Echoes from a clutter patch after conversion to baseband for $N = 2$, $\bar{N} = 3$, and $\zeta = \bar{\zeta}$

Another example involving a pulse-compression waveform and a single target is shown in Fig. 6. The target echoes are shown delayed by both the matched-filter and range delays. The central peak between zero crossings of the compressed pulse is shown to width 2ζ so that the pulse-compression ratio is approximately $\bar{\zeta}/\zeta$.

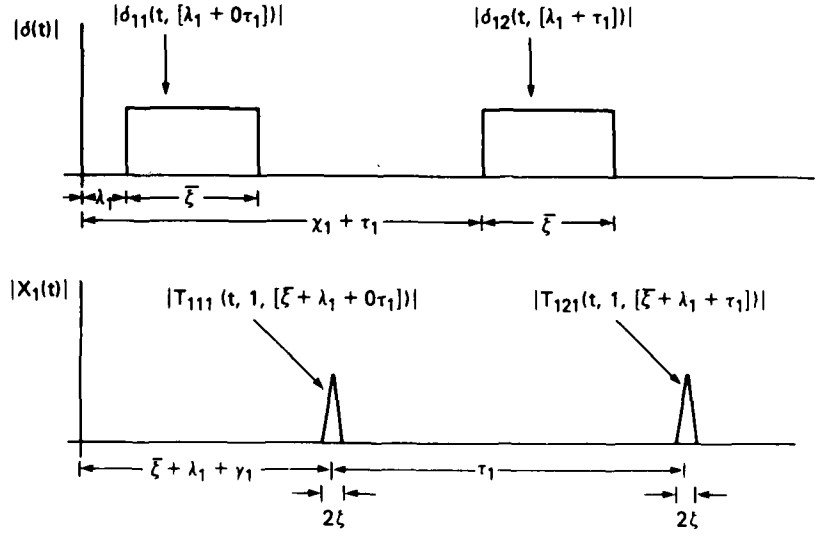

Fig. 6 — Target echoes after conversion to baseband for $N = 1$, $\bar{N} = 2$, and $\zeta \neq \bar{\zeta}$

Transversal Filters

The Doppler processing of the received signals is performed in a conventional manner with transversal filters [1]. The process is defined by

$$Y_p(t, \mathrm{v}, [0]) = \sum_{m=1}^{M} W_{p\mathrm{v}m} X_p(t, [\tau_{pm}]), \tag{6}$$

where $Y_p(t, \mathrm{v}, [0])$ is the complex Doppler-filtered signals (passed through 0 circuit delays) of the pth and vth filter, with $p = 1, 2, \ldots, N$ and $\mathrm{v} = 1, 2, 3, \ldots, N_\mathrm{v}$, N_v being the number of outputs for each pth signal, M is the order of the filter, $W_{p\mathrm{v}m}$ is the mth filter weight of the pth and vth filter, and τ_{pm} is the circuit time delay of the mth filter tap of the pth filter. Again, the arguments in brackets [0] and $[\tau_{pm}]$ indicate that the signals $Y_p(t, \mathrm{v})$ have no new delays beyond the delay τ_{pm} already present in the signal $X_p(t)$. The signal flow for the filters is shown in Fig. 7, and the form of the pth and vth filter is shown in Fig. 8. The filters can be used as band-rejection filters, which are conventionally used in MTI radar systems, or as bandpass filters, which are conventionally used in pulse-Doppler radar systems. This is accomplished by adjusting the filter weights $W_{p\mathrm{v}m}$. The circuit time delays in the pth filter are all identical. Consequently the time delays τ_{pm} can be written as

$$\tau_{pm} = (m - 1)\, \tau_p,$$

where the time delays τ_p are set equal to the interpulse spacing τ_i for $i = p$:

$$\tau_p = \tau_i, \quad \text{for } i = p.$$

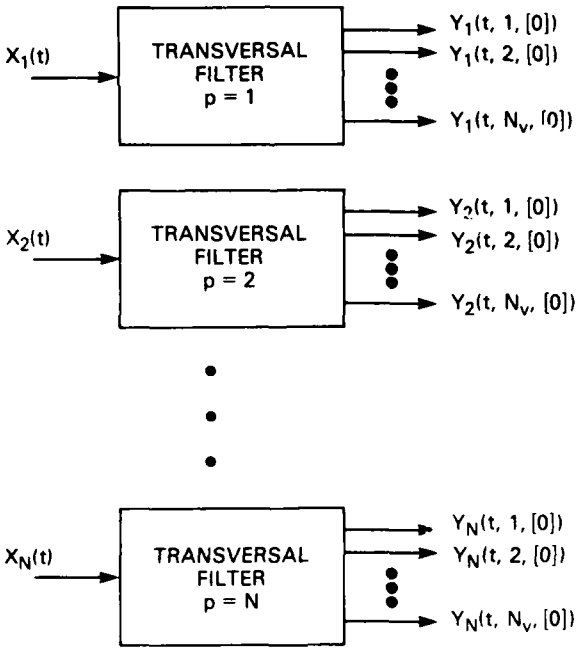

Fig. 7 — Signal flow for the Doppler filters

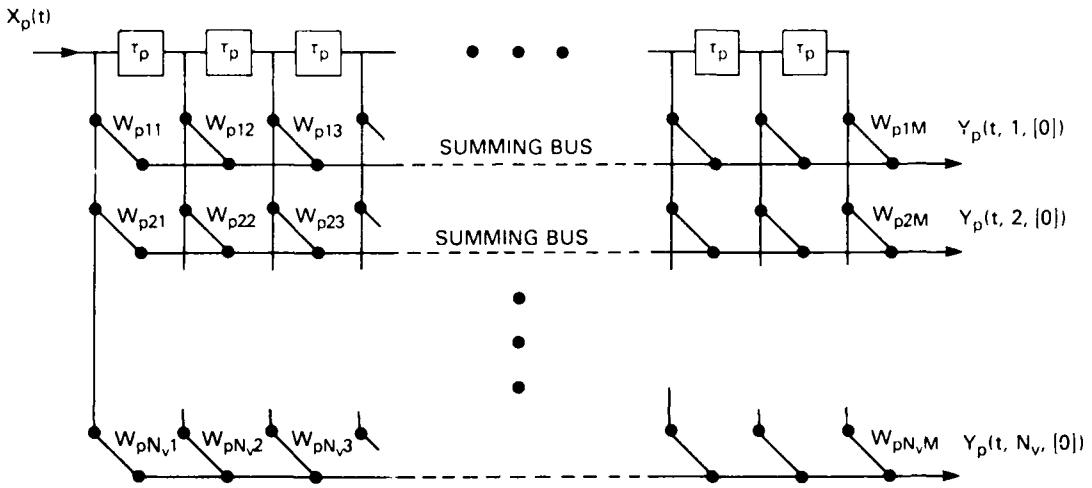

Fig. 8 — Form of the pth and vth transversal filter

The complex Doppler-filtered signals are written in terms of the complex baseband signals by combining Eqs. (3) through (6), yielding

$$Y_p(t, v, [0]) = \sum_{k=1}^{N_c}\sum_{m=1}^{M}\sum_{i=1}^{N}\sum_{j=1}^{\bar{N}} W_{pvm} C_{ijp}(t, k, [\bar{\zeta} + \lambda_i + (j-1)\tau_i + (m-1)\tau_p])$$
$$+ \sum_{l=1}^{N_t}\sum_{m=1}^{M}\sum_{i=1}^{N}\sum_{j=1}^{\bar{N}} W_{pvm}\, T_{ijp}(t, l, [\bar{\zeta} + \lambda_i + (j-1)\tau_i + (m-1)\tau_p])$$
$$+ \sum_{m=1}^{N} W_{pvm}\, N_p(t), \tag{7}$$

where the order of summations has been changed and the circuit time delays have been added together.

An example is illustrated in Fig. 9. Two pulse trains $N = 2$ containing $\bar{N} = 3$ pulses each are transmitted at identical frequencies but separated in time. The echoes are assumed to have no Doppler shift so that the single target echoes are all of amplitude $|A|$, where A is a complex number of fixed phase for all six echoes. The filter is of the order of $M = 2$, and all the weights are $1 + \hat{j}0$. No clutter or noise is present. The resulting waveforms before and after filtering are shown in Fig. 9. Filter 1 is matched to the first pulse train; consequently filter 1 gives an unusable output to the second pulse train, because the time delays in the filter do not match the pulse spacing in the pulse train. A similar result is obtained for all pulse trains not matched to the filter. When the pulse trains pulse spacing does match the filter time delays, the desired response is obtained. The desired response has a leading and trailing transient condition with a steady state condition in between. In the example given the first response in $|Y_1(t, v, [0])|$ is a value $|A|$ which comes from the first target echo. This is a transient condition, because the entire filter is not yet loaded. The filter reaches a steady-state condition on the next two pulses, and then again a transient condition exists as the last pulse exits the filter.

Time Alignment

For convenience as well as for target ranging, the complex Doppler-filtered signals are passed through a time-alignment circuit consisting of multiple sets of delay lines. The linear operation we require is defined by

$$Z_{pq}(t, v) = Y_p(t, v, [(\lambda_N - \lambda_p) + (\bar{\tau} - \tau_p)(q-1) + \bar{\tau}(\bar{N} + M - 1 - q)]), \tag{8}$$

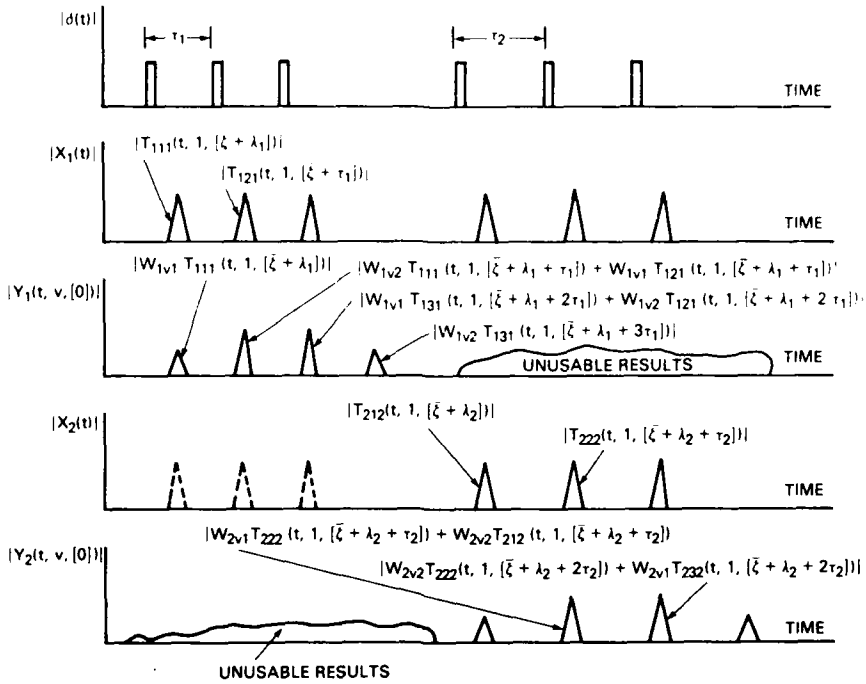

Fig. 9 — Complex Doppler filtered signals $Y_p(t, v, 0)$ for the case of $N = 2$, $\bar{N} = 3$, and $M = 2$, all weights $W_{prm} = 1$, all target echoes identical, and no noise present

where $p = 1, 2, \ldots, N$, $q = 1, 2, \ldots, (\bar{N} + M - 1)$, $v = 1, 2, \ldots, N_v$, and $Z_{pq}(t, v)$ is the time-aligned Doppler-filtered signal from the vth filter appearing at the pth and qth tap of the delay lines. The operation using delay lines is illustrated in Fig. 10.

By combining Eqs. (7) and (8), the time-aligned Doppler-filtered signals are expressed in terms of the complex baseband signals by

$$
\begin{aligned}
Z_{pq}(t, v) = & \sum_{k=1}^{N_c} \sum_{m=1}^{M} \sum_{i=1}^{N} \sum_{j=1}^{\bar{N}} W_{pvm}\, C_{ijp}(t, k, [\bar{\zeta} + \lambda_i + (j-1)\tau_i + (m-1)\tau_p + (\lambda_N - \lambda_p) \\
& + (\bar{\tau} - \tau_p)(q-1) + \bar{\tau}(\bar{N} + M - 1 - q)]) \\
& + \sum_{l=1}^{N_l} \sum_{m=1}^{M} \sum_{i=1}^{N} \sum_{j=1}^{\bar{N}} W_{pvm}\, T_{ijp}(t, l, [\bar{\zeta} + \lambda_i + (j-1)\tau_i + (m-1)\tau_p + (\lambda_N - \lambda_p) \\
& + (\bar{\tau} - \tau_p)(q-1) + \bar{\tau}(\bar{N} + M - 1 - q)]) \\
& + \sum_{m=1}^{M} W_{pvm}\, N_p(t, [(\lambda_N - \lambda_p) + (\bar{\tau} - \tau_p)(q-1) + \bar{\tau}(\bar{N} + M - 1 - q)]),
\end{aligned}
\tag{9}
$$

where the circuit time delays have been added together. Furthermore we define the signal $Z_{pq}(t, v)$ to be composed of three additive signal components given by

$$
Z_{pq}(t, v) = \tilde{Z}_{pq}(t, v) + \bar{Z}_{pq}(t, v), + \hat{Z}_{pq}(t, v), \tag{10}
$$

where the signals in $\tilde{Z}_{pq}(t, v)$ are composed of complex baseband signals derived only from the echoes due to the ith pulse train passing through the $p = i$th receiver, the signals $\bar{Z}_{pq}(t, v)$ are due to only the noise, and the signals in $\hat{Z}_{pq}(t, v)$ are composed of all other complex baseband signals except those due

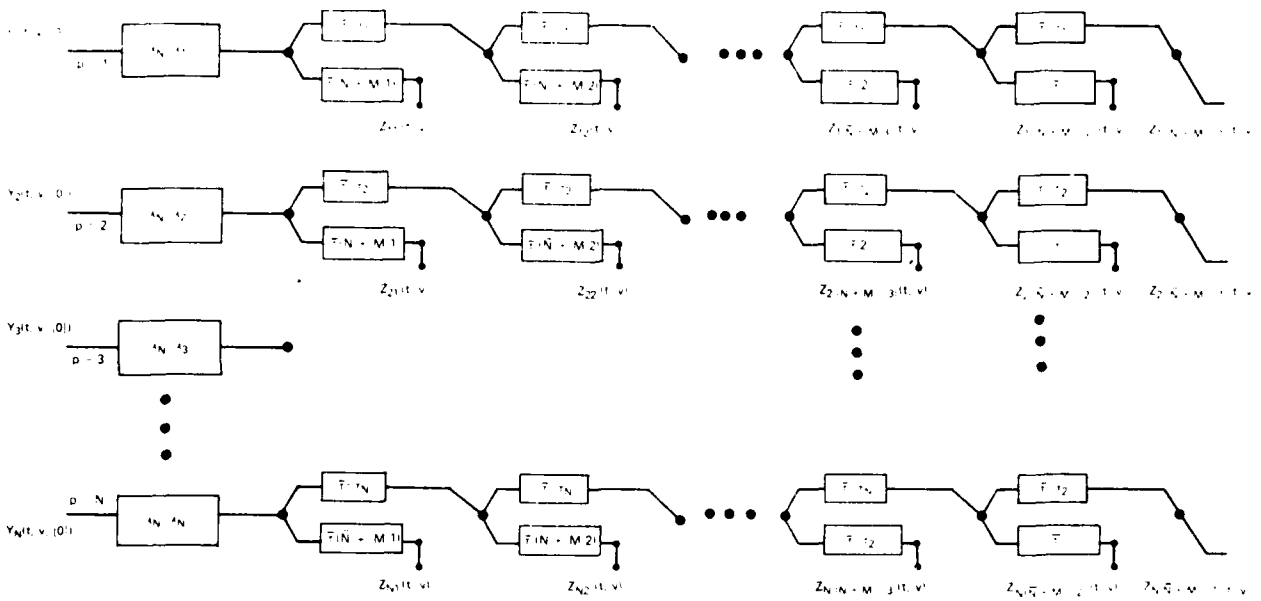

Fig. 10 — Schematic representation of the time-alignment circuit for filtered radar echoes from the vth filter

to noise and those echoes due to the ith pulse train passing through the $p = i$ receiver. By use of Eq. (9), the signal $\hat{Z}_{pq}(t, \mathrm{v})$ is

$$\hat{Z}_{pq}(t, \mathrm{v}) = \sum_{k=1}^{N_c} \sum_{m=1}^{M} \sum_{\substack{i=1 \\ i \neq p}}^{N} \sum_{j=1}^{\bar{N}} W_{p\mathrm{v}m}\, C_{ijp}(t, k, [\bar{\zeta} + \lambda_i + (j-1)\tau_i + (m-1)\tau_p + (\lambda_N - \lambda_p) + (\bar{\tau} - \tau_p)(q-1) + \bar{\tau}(\bar{N} + M - 1 - q)])$$

$$+ \sum_{l=1}^{N_t} \sum_{m=1}^{M} \sum_{\substack{i=1 \\ i \neq p}}^{N} \sum_{j=1}^{\bar{N}} W_{p\mathrm{v}m}\, T_{ijp}(t, l, [\bar{\zeta} + \lambda_i + (j-1)\tau_i + (m-1)\tau_p + (\lambda_N - \lambda_p) + (\bar{\tau} - \tau_p)(q-1) + \bar{\tau}(\bar{N} + M - 1 - q)]), \tag{11}$$

the signal $\bar{Z}_{pq}(t, \mathrm{v})$ is

$$\bar{Z}_{pq}(t, \mathrm{v}) = \sum_{m=1}^{M} W_{p\mathrm{v}m}\, N_p(t, [(\lambda_N - \lambda_p) + (\bar{\tau} - \tau_p)(q-1) + \bar{\tau}(\bar{N} + M - 1 - q)]), \tag{12}$$

and the signal $\tilde{Z}_{pq}(T, \mathrm{v})$ is

$$\tilde{Z}_{pq}(t, \mathrm{v}) = \sum_{k=1}^{N_c} \sum_{m=1}^{M} \sum_{j=1}^{\bar{N}} W_{p\mathrm{v}m}\, C_{pjp}(t, k, [\bar{\zeta} + \lambda_N + (\bar{N} + M - 2)\bar{\tau} + (j + m - 2)\tau_p - (q-1)\tau_p])$$

$$+ \sum_{l=1}^{N_t} \sum_{m=1}^{M} \sum_{j=1}^{\bar{N}} W_{p\mathrm{v}m}\, T_{pjp}(t, l, [\bar{\zeta} + \lambda_N + (\bar{N} + M - 2)\bar{\tau} + (j + m - 2)\tau_p - (q-1)\tau_p]). \tag{13}$$

The understanding of the structure and properties of the component $\tilde{Z}_{pq}(t, v)$ of the time-aligned Doppler-filtered signals represented by Eq. (13) is a major thrust of the study to be presented.

The time-alignment operation is defined so that echoes from a single target will cause nonzero signals to be simultaneously present over a time ζ in $\tilde{Z}_{pq}(t, v)$ for all permissible values of p and q when the transmitter transmits all $N \cdot \bar{N}$ pulses. The reason for this requirement and the proof that the time-alignment operator matches this requirement is discussed later. However, knowing the requirement allows us to discuss, in the next paragraph, why q takes on values up to $\bar{N} + M - 1$.

After a target echo due to the first pulse of the ith pulse train passed through the $(p = i)$th receiver becomes present in the filter, the filter responds to each subsequent echo until a steady-state condition is reached at the time of the target echo due to the Mth pulse. A steady-state condition of the filter is maintained until after the target echo due to the last transmitted pulse (the $\bar{N}$th pulse of the ith pulse train) is processed. At this point the filter continues to have an output in $M - 1$ time locations even though there is no input target echo. Consequently there are $\bar{N} + M - 1$ filter responses due to echoes from a single target and the ith pulse train which are passed through the $p = i$th receiver. For any given target and any ith pulse train, there are $M - 1$ filter responses at the beginning and the end of the total set of filtered responses in which the filter is in a transient state, and there are $\bar{N} - M + 1$ filter responses in which the filter is in a steady-state condition.

An example of the time-alignment operation is illustrated in Fig. 11. The input signals are shown in Fig. 9. The pulse trains shown for $Z_{pq}(t, v)$ are the components of $\tilde{Z}_{pq}(t, v)$, and the regions of time in Fig. 9 labeled "unusable results" are the components of $\tilde{Z}_{pq}(t, v)$. The noise component $\bar{Z}_{pq}(t, v)$ is zero. One time exists when all the processed echoes in $\tilde{Z}_{pq}(t, v)$ from a single target are brought into time alignment, which is the desired result.

Target Detector

The target detection and measurement process will not be of concern in the study and thus will not be discussed in depth in setting the stage for presenting the study. However, it is defined so that the form of all the signal processors are described before we develop the basic theorems and describe conventional pulse-Doppler and MTI operations. The basic detector is constructed from a series of three operations. First the outputs of the time-alignment operation $Z_{pq}(t, v)$ are passed through a conventional CFAR detector expressed by

$$D_{pq}(t, v) = \begin{cases} 1, & \text{if } Z_{pq}(t, v) > \sigma_{pq}(t) \times \psi_1(t), \\ 0, & \text{otherwise,} \end{cases}$$

for $p = 1, 2, \ldots, N$, $q = 1, 2, \ldots, (\bar{N} + M - 1)$, and $v = 1, 2, \ldots, N_v$ where $\sigma_{pq}(t)$ is the CFAR normalization parameter which requires estimation, $\psi_1(t)$ is the first threshold, and $D_{pq}(t, v)$ is the detector output, which is 1 if a signal is present above the background at the pqth tap of the time-alignment circuit and is 0 if no signal is present. The second operation is involved in counting the number of simultaneous target detections obtained from the outputs of the time-alignment operation. The process is defined by

$$D(t, v, \mu) = \begin{cases} 1, & \text{if } \sum_{p=1}^{N} \sum_{q=1}^{\bar{N}+M-1} \theta_{pq}(t, \mu) D_{pq}(t, v) > \psi_2(t), \\ 0, & \text{otherwise,} \end{cases}$$

for $\mu = 1, 2, \ldots, N_\mu$ and $v = 1, 2, \ldots, N_v$, where $\theta_{pq}(\mu, t)$ is a function which takes on values of 0 and 1, $\psi_2(t)$ is the second threshold, N_μ is the number of second detector operations, and $D(t, v, \mu)$ is the output of the second detector operation which takes on a value of 0 or 1. Finally the third detector operation is an operation defined on the output of the second operation, and several possibilities exist. An example of third detector operation is

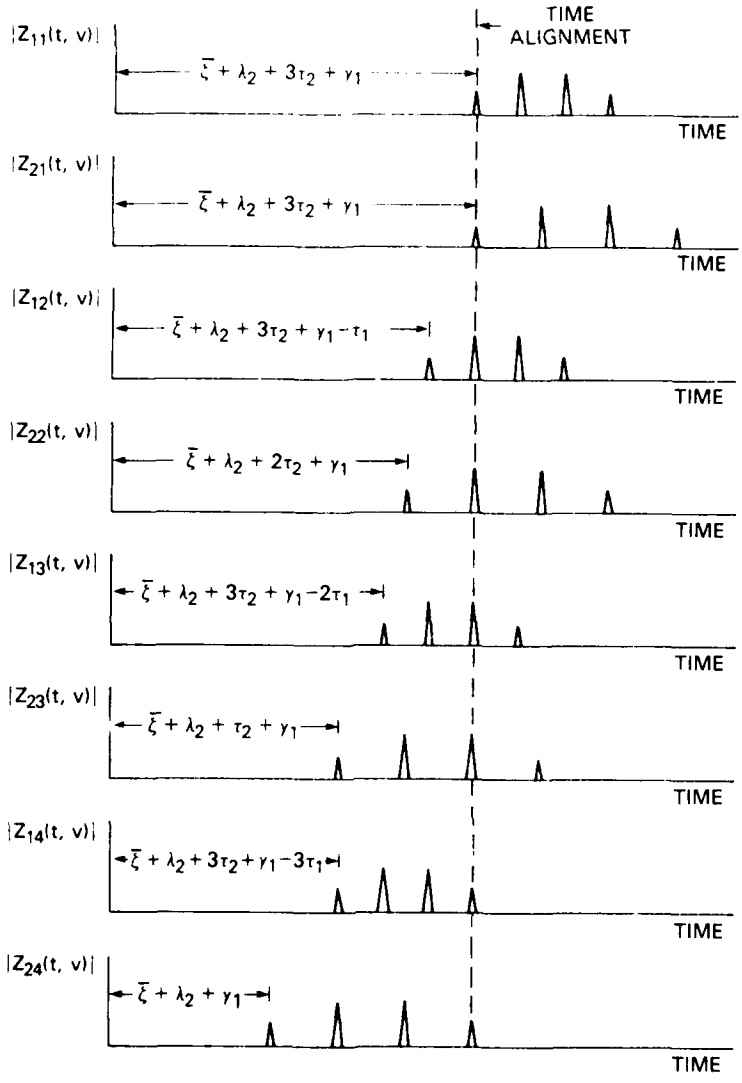

Fig. 11 — Time-alignment operation performed on the complex Doppler-filtered signals of Fig. 9

$$D(t, \mathrm{v}) = \begin{cases} 1, & \text{if } \bigcap_{\mu=1}^{N_\mu} D(t, \mathrm{v}, \mu) > \psi_3(t), \\ 0, & \text{otherwise,} \end{cases}$$

for v = 1, 2, ..., N_v, where $\cap$ is the logic *and* operator, $\psi_3(t)$ is the threshold of the third detector operation, and $D(t, \mathrm{v})$ is the detection history for each of the vth Doppler filters as a function of time.

The detector operations may be interpreted as follows. The first operation is concerned with obtaining the detection of signals above the background for all outputs of the time-alignment operation. The next two detector operations are concerned with allowing only a final target declaration for a specified distribution of detections made by the first detector across the $p = 1, 2, \ldots, N$ and $q = 1, 2, \ldots, \bar{N} + M - 1$ outputs of the time-alignment circuit. For example the second detector could require coincident detections for all values of p as q takes on different values $\mu = q$. The third detector could

then require $\mu = \tilde{\mu}$ of the outputs of the second detector to be present. If a pq matrix of first detections were constructed, we would find $\tilde{\mu}$ columns with all values being 1 if a final target declaration was made for this example. The data flow in the detector and the processes involved are represented pictorially in Fig. 12.

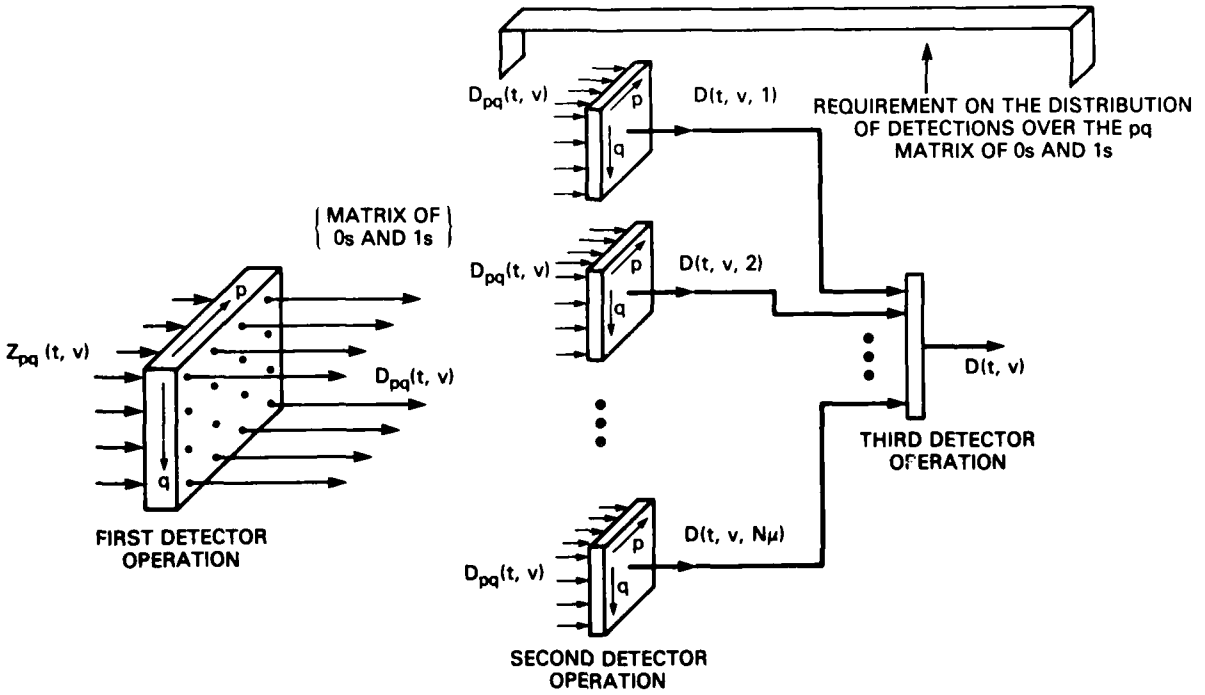

Fig. 12 — Functional operations of a detector

Although we have not discussed the material required to fully understand the detection process, we can make a few brief comments concerning the detector. First, clutter conditions exist for which targets are masked in some of the outputs of the time-alignment operation. Consequently only certain subsets of the outputs of the time-alignment circuits will contain detectable signal levels due to targets. Second, there is a tradeoff between the probability of detecting real targets and the probability of detecting ghost targets. This tradeoff is controlled by the second and third operations of the detector, which control the requirements on the distribution of detections over the outputs of the time-alignment operation. A ghost-target condition exists when a target declaration is made which is due to the echoes of multiple targets at different ranges. The form of the detector was chosen to balance the real-target and ghost-target detections when targets are visible over a portion of the time-alignment circuits.

Once a final target declaration is made, the target's range and angle of arrival are determined. Both are determined in a conventional manner. The range is determined by measuring the time delay (proportional to range) between the first transmitted pulse and the target detection and subtracting off a fixed circuit bias. The angle is recorded at the time of the target detection.

BASIC THEOREMS AND DEFINITIONS

We now define frequency and time orthogonality conditions between pulse trains. The processors we will describe that will be involved in the study will require at least one of the two conditions for proper operation. The basic theorem underlying such operation we will then state and prove. This

theorem simply involves the rearrangement of terms in the representation of the signals. Some other theorems and definitions which are independent of a specific Doppler processor are next given.

Orthogonality Conditions

The frequency orthogonality condition is defined as follows:

Definition: The pulse trains are said to meet the frequency orthogonality condition if $\hat{Z}_{pq}(t, \nu)$ is below the thermal noise for all p, q, and ν even for the very strongest echo conditions. This implies that the pulse trains are offset in frequency ω_i enough so that good filtering can separate them.

The time orthogonality condition is defined as follows:

Definition: The pulse trains are said to meet the time orthogonality condition if $\hat{Z}_{p\,q}(t, \nu)$ and $\tilde{Z}_{p\,q}(t, \nu)$ do not occur over the same time. This condition is met if any two pulse trains are separated in time enough. The condition is stated in the following lemma.

Lemma 1: The time orthogonality condition is met if

$$(\lambda_{i+1} - \lambda_i) > (\bar{N} - 1)\,\tau_i + \max \begin{Bmatrix} \beta_{N_c} \\ \gamma_{N_t} \end{Bmatrix} - \min \begin{Bmatrix} \alpha_1 \\ \gamma_1 \end{Bmatrix}, \quad \text{for all } i,$$

where $\max \begin{Bmatrix} \beta_{N_c} \\ \gamma_{N_t} \end{Bmatrix}$ is the time equivalent of the range to the farthest expected echo and $\min \begin{Bmatrix} \alpha_i \\ \gamma_1 \end{Bmatrix}$ is the time equivalent of the range to the nearest echo. This lemma is proved in Appendix A.

Rearrangement Theorem

The rearrangement theorem, which is fundamental to processor operation in the study, involves rearranging the terms describing $\tilde{Z}_{pq}(t, \nu)$ and defining new signals which are components of $\tilde{Z}_{pq}(t, \nu)$. The theorem is as follows:

Rearrangement Theorem: The signal $\tilde{Z}_{pq}(t, \nu)$ can be written as

$$\tilde{Z}_{pq}(t, \nu) = \tilde{Z}^T_{pq}(t, \nu) + \tilde{Z}^c_{pq}(t, \nu),$$

where

$$\tilde{Z}^T_{pq}(t, \nu) = \sum_{l=1}^{N_t} [\overset{<}{R}{}^T_{pq}(t, \nu, l) + S^T_{pq}(t, \nu, l) + \overset{>}{R}{}^T_{pq}(t, \nu, l)]$$

and

$$\tilde{Z}^c_{pq}(t, \nu) = \sum_{k=1}^{N_c} [\overset{<}{R}{}^c_{pq}(t, \nu, k) + S^c_{pq}(t, \nu, k) + \overset{>}{R}{}^c_{pq}(t, \nu, k)],$$

in which

$$\overset{<}{R}{}^T_{pq}(t, \nu, l) = \sum_{j'=1}^{M-1} \sum_{m=1}^{j'} W_{p\nu m}\, T_{p(j'-m+1)p}\,(t, l, [\bar{\zeta} + \lambda_N + (\bar{N} + M - 2)\,\bar{\tau}$$

$$+ (j' - 1)\tau_p - (q - 1)\,\tau_p]),$$

$$S^T_{pq}(t, v, l) = \sum_{j'=M}^{\bar{N}} \sum_{m=1}^{M} W_{pvm}\, T_{p(j'-m+1)p}\,(t, l, [\bar{\zeta} + \lambda_N + (\bar{N} + M - 2)\,\bar{\tau} + (j' - 1)\,\tau_p - (q - 1)\,\tau_p]),$$

$$\overset{>}{R}{}^T_{pq}(t, v, l) = \sum_{j'=\bar{N}+1}^{\bar{N}+m-1} \sum_{m=j'-\bar{N}+1}^{M} W_{pvm}\, T_{p(j'-m+1)p}\,(t, l, [\bar{\zeta} + \lambda_N + (\bar{N} + M - 2)\bar{\tau} + (j' - 1)\tau_p - (q - 1)\tau_p]),$$

$$\overset{<}{R}{}^c_{pq}(t, v, k) = \sum_{j'=1}^{M-1} \sum_{m=1}^{j'} W_{pvm}\, C_{p(j'-m+1)p}\,(t, k, [\bar{\zeta} + \lambda_N + (\bar{N} + M - 2)\tau + (j' - 1)\tau_p - (q - 1)\tau_p]),$$

$$S^c_{pq}(t, v, k) = \sum_{j'=M}^{\bar{N}} \sum_{m=1}^{M} W_{pvm}\, C_{p(j'-m+1)p}\,(t, k, [\bar{\zeta} + \lambda_N + (\bar{N} + M - 2)\bar{\tau} + (j' - 1)\tau_p - (q - 1)\tau_p]),$$

$$\overset{>}{R}{}^c_{pq}(t, v, k) = \sum_{j'=\bar{N}+1}^{\bar{N}+M-1} \sum_{m=j'-\bar{N}+1}^{M} W_{pvm}\, C_{p(j'-m+1)p}\,(t, k, [\bar{\zeta} + \lambda_N + (\bar{N} + M - 2)\bar{\tau} + (j' - 1)\tau_p - (q - 1)\tau_p]).$$

The proof of this theorem is given in Appendix A. We define $\tilde{Z}^T_{pq}(t, v)$ and $\tilde{Z}^c_{pq}(t, v)$ as components of $Z_{pq}(t, v)$ due to targets and clutter respectively. We define $\overset{<}{R}{}^T_{pq}(t, v, l)$ and $\overset{<}{R}{}^c_{pq}(t, v, k)$ as left remainder signals for targets and clutter respectively. We define by $S^T_{pq}(t, v, l)$ and $S^c_{pq}(t, v, k)$ as separation signals for targets and clutter respectively. We define $\overset{>}{R}{}^T_{pq}(t, v, l)$ and $\overset{>}{R}{}^c_{pq}(t, v, k)$ as right remainder signals for targets and clutter respectively. All the right remainder, separation, and left remainder signals appear at the pqth tap of the time-alignment circuit for the vth filter. The j' index represents the counting of the number of filtered target echoes from a single target starting with the first one and ending with the last one as the filter decays to zero. The index range $j' = 1$ to $M - 1$ represents the filter's transient signals, the index range $j' = M$ to $\bar{N}$ represents the filter's steady-state signals, and the index range $j' = \bar{N} + 1$ to $\bar{N} + M - 1$ represents the filter's decaying signals for a given target or clutter. The left remainder signals for any one target or clutter is composed of terms for when the filter is in a transient state during the initial buildup. The separation signals for any one target or clutter is composed of terms for when the filter is in a steady-state condition. The right remainder signals for any one target or clutter is composed of terms for when the filter response is decaying. The example shown in Fig. 11 is repeated in Fig. 13 with the separation and remainder signals labeled.

Separation Time Intervals

The concept of separation time intervals is defined on pulse trains meeting either the time orthogonality condition or the frequency orthogonality condition. The kth-clutter-patch separation time interval for the pth pulse train denoted by Δ^c_{kp} is defined with the aid of Fig. 14 as follows. First time is broken into intervals of length τ_p beginning at the time of the leading edge of the first transmitted pulse in the first pulse train. The left edge of Δ^c_{kp} is then defined as the first time interval of length τ_p which occurs after the time interval containing the trailing edge of $\overset{<}{R}{}^c_{pq}(t, \nu, k)$ and is given by

$$\text{integer}\left\{\frac{\beta_k + \chi_{pq}}{\tau_p}\right\}\tau_p + \tau_p + (M - 2)\tau_p.$$

where

$$\chi_{pq} = \bar{\zeta}_t + \lambda_N + (\bar{N} + M - 2)\bar{\tau} - (q - 1)\tau_p.$$

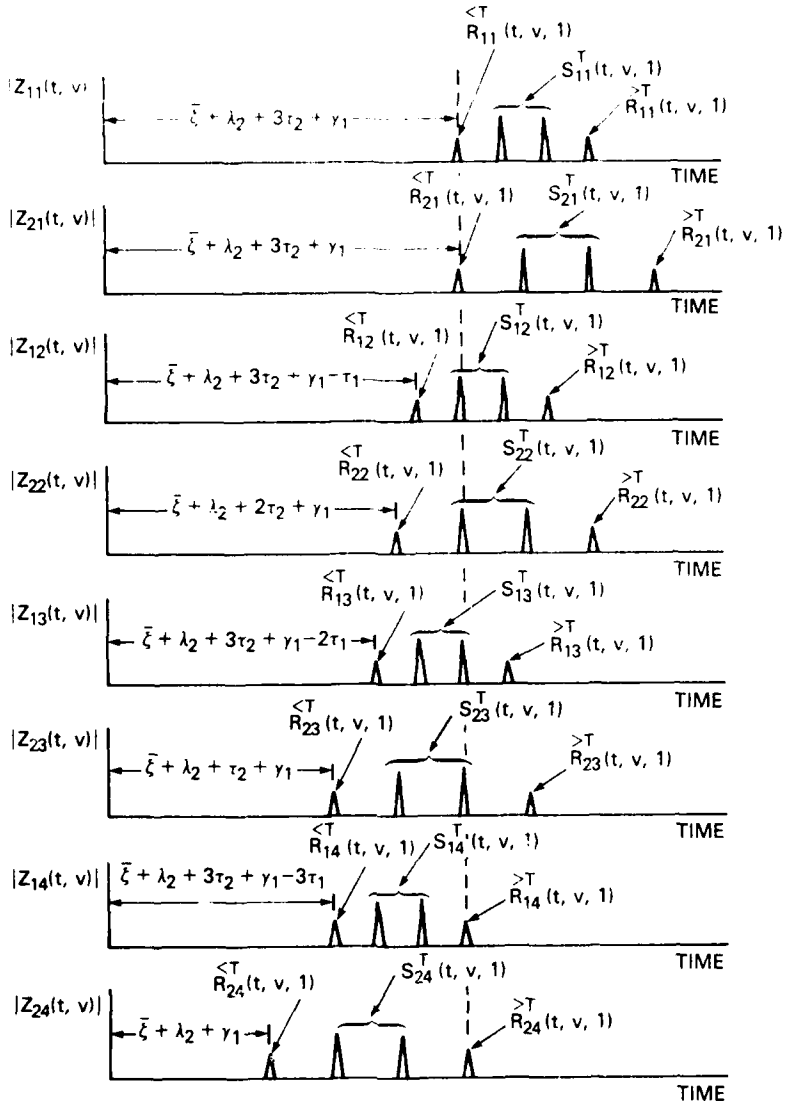

Fig. 13 — Remainder and separation signals for the example shown in Fig. 11

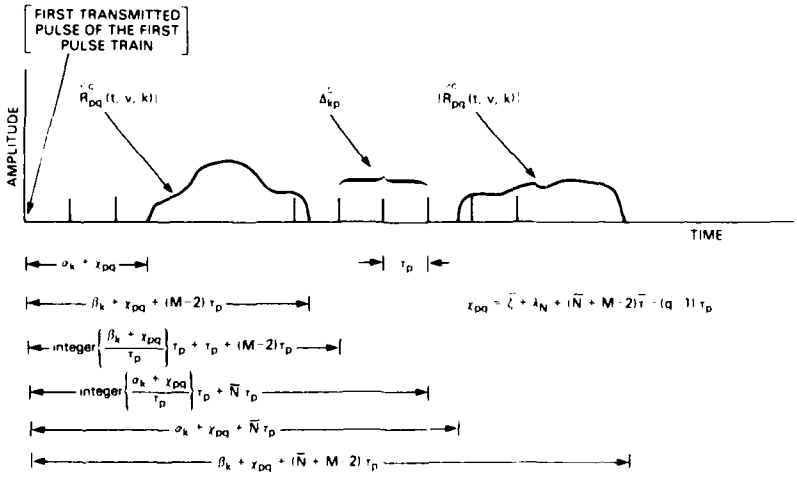

Fig. 14 — The kth-clutter-patch separation time for the pth pulse train Δ^{c}_{kp}

The right edge of Δ_{kp}^{c} is defined as the last time interval of length τ_p which occurs before the time interval containing the leading edge of $\overset{>}{R}_{pq}^{c}(t, \nu, k)$ and is given by

$$\text{integer}\left\{\frac{\alpha_k + \chi_{pq}}{\tau_p}\right\}\tau_p + \bar{N}\tau_p.$$

Subtracting the left edge from the right edge gives the width of the kth-clutter-patch separation time interval for the pth pulse train as

$$\text{integer}\left\{\frac{\alpha_k + \chi_{pq}}{\tau_p}\right\}\tau_p - \text{integer}\left\{\frac{\beta_k + \chi_{pq}}{\tau_p}\right\}\tau_p + (\bar{N} - M + 1)\tau_p.$$

Similarly, the lth target separation time interval for the pth pulse train denoted by Δ_{lp}^{T} is defined with the aid of Fig. 15 as follows. Again time is broken into intervals of length τ_p beginning at the time of the leading edge of the first transmitted pulse in the first pulse train. The left edge of Δ_{lp}^{T} is then defined as the first time interval of length τ_p which occurs after the time interval containing the trailing edge of $\overset{<}{R}_{pq}^{T}(t, \nu, k)$ and is given by

$$\text{integer}\left\{\frac{\gamma_l + \chi_{pq} + \bar{\zeta}_i}{\tau_p}\right\}\tau_p + \tau_p + (M - 2)\tau_p.$$

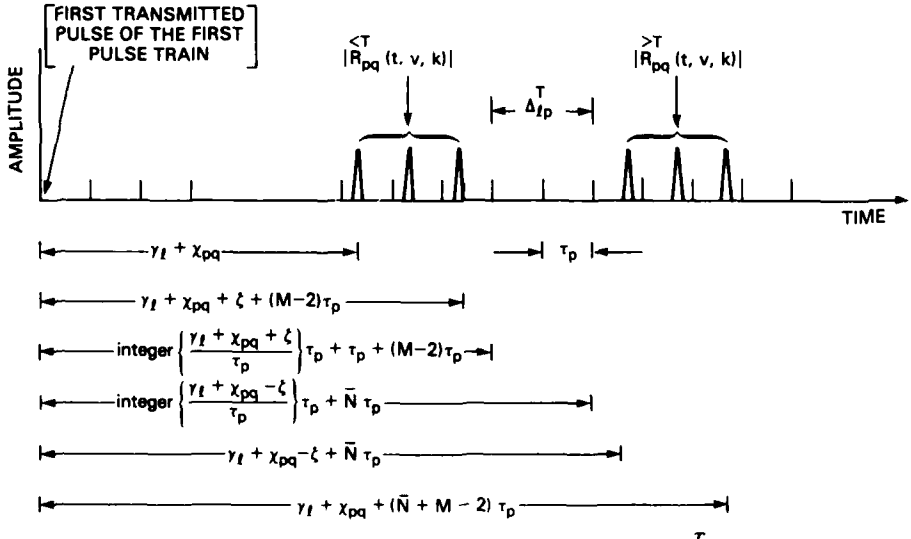

Fig. 15 — The lth target separation time interval Δ_{lp}^{T}

The right edge of Δ_{lp}^{T} is defined as the last time interval of length τ_p which occurs before the time interval containing the leading edge of $\overset{>}{R}_{pq}^{T}(t, \nu, k)$ and is given by

$$\text{integer}\left\{\frac{\gamma_l + \chi_{pq} - \bar{\zeta}_i}{\tau_p}\right\} + \bar{N}\tau_p.$$

Subtracting the left edge from the right edge gives the width of the kth-clutter-patch separation time interval for the pth pulse train as

$$\text{integer}\left\{\frac{\gamma_l + \chi_{pq} - \bar{\zeta}_i}{\tau_p}\right\}\tau_p - \left\{\frac{\gamma_l + \chi_{pq} + \bar{\zeta}_i}{\tau_p}\right\}\tau_p + (\bar{N} - M + 1)\tau_p.$$

We next state the separation-time-interval theorem, which will be used later.

Separation-Time-Interval Theorem: The filter is in steady-state operation over the kth-clutter-patch separation time interval for echoes from the kth clutter patch due to the $(p = i)$th pulse train. Similarly the filter is in steady-state operation over the lth-target separation time interval for echoes from the lth target due to the $(p = i)$th pulse train.

The proof of the theorem is given in Appendix A. This theorem is almost trivial but serves as the basis of the rest of this report. Furthermore we find the filter can obtain steady-state operation locally over a clutter patch. We will more fully exploit this fact subsequently.

The two cases which arose in the theorem proof are illustrated in Figs. 16 and 17. In Fig. 16, part of the steady-state separation signal is covered by the remainder signal, but the steady-state filter condition exists over the kth-clutter-patch separation time interval. In Fig. 17, the steady-state separation signal exists over only portions of the kth-clutter-patch separation time interval, and none of it is covered by the remainder signals.

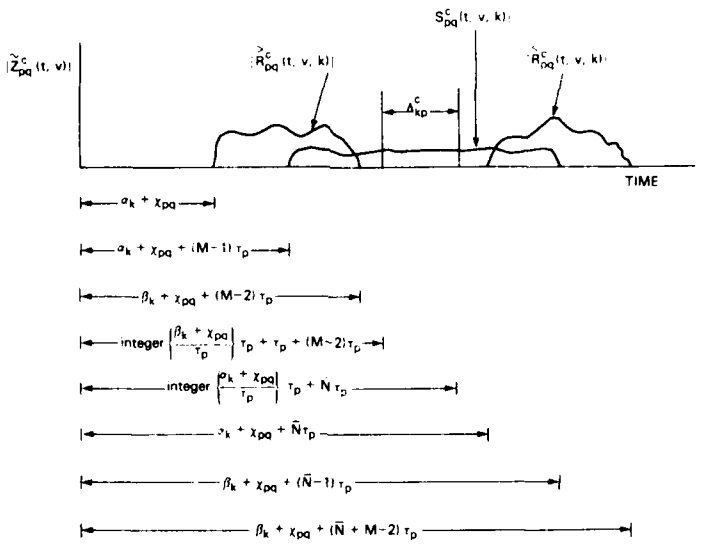

Fig. 16 — Time frames for the clutter remainder and separation signal for $(\beta_k - \alpha_k) > \tau_p$ for the kth clutter patch and the pth pulse train

Time-Alignment Theorem

We are now in a position to state that the time-alignment operation defined earlier does in fact perform the desired operation. We restate the operation as a theorem, with the proof being given in Appendix A:

Time-Alignment Theorem: The filtered radar echo from a single target due to the jth pulse of the ith pulse train appears in $\tilde{Z}_{pq}(t, v)$ for $p = i$ and $q = j'$ at a time $\lambda_N + \bar{\tau}(\bar{N} + M - 2)$. This is true for all values of $i = 1, 2, \ldots, N$ and $j' = 1, 2, \ldots, \bar{N} + M - 1$.

Segmented Clutter Signals

A well-known fact about pulse-Doppler radars is that when the range is ambiguous due to the clutter extent and the pulse-repetition rate, the clutter echoes from multiple ranges are superimposed.

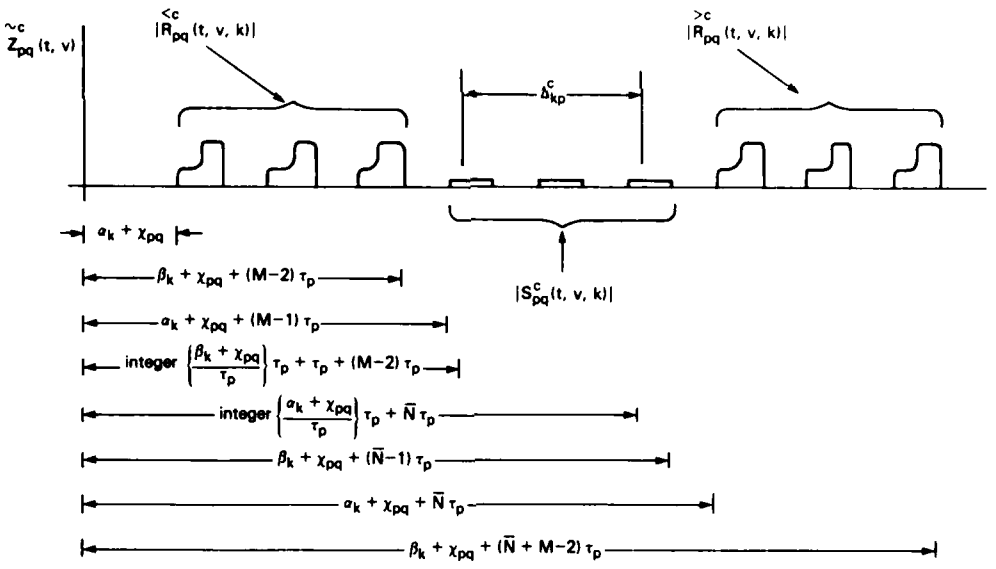

Fig. 17 — Time frames for the clutter remainder and separation signals for $(\beta_k - \alpha_k) < \tau_p$ for the kth clutter patch and the pth pulse train

Subsequently we will prove theorems concerning this property. In the interim, however, it is useful to define a segmented clutter signal:

Definition of a Segmented Clutter Signal: If the time interval required to transmit the ith pulse train, which meets either the frequency orthogonality condition or the time orthogonality condition, is larger than the time extent of the kth clutter echo, then the kth clutter echo can be broken into time intervals of width τ_i and the kth clutter echo can be expressed by

$$C_{p(j'-m+1)p}(t,\ k,\ [\chi_{pq} + (j'-1)\tau_p]) = \sum_{\mu=1}^{N_k} \tilde{C}_{p(j'-m+1)p}\left(t,\ k,\ \mu,\ \left[\text{integer}\left\{\frac{\alpha_k + \chi_{pq}}{\tau_p}\right\}\tau_p + (j'-1)\tau_p + (\mu-1)\tau_p\right]\right),$$

where the μth segmented clutter signal is

$$\tilde{C}_{p(j'-m+1)p}\left(t,\ k,\ \mu,\ \left[\text{integer}\left\{\frac{\alpha_k + \chi_{pq}}{\tau_p}\right\}\tau_p + (j'-1)\tau_p + (\mu-1)\tau_p\right]\right)$$

and is the same as

$$C_{p(j'-m+1)p}(t,\ k,\ [\chi_{pq} + (j'-1)\tau_p])$$

over the time interval from $(\mu-1)\tau_p$ to $\mu\tau_p$. The time interval from $(\mu-1)\tau_p$ to $\mu\tau_p$ is defined for $\mu = 1$ as the first time segment of length τ_p containing α_k. Furthermore N_k is

$$N_k = \text{integer}\left\{\frac{\beta_k + \chi_{pq}}{\tau_p}\right\} - \text{integer}\left\{\frac{\alpha_k + \chi_{pq}}{\tau_p}\right\} + 1,$$

where again the integer function simply means that the fractional part of the rational number is ignored.

The μth segmented clutter is illustrated in Fig. 18. The figure shows that segmented clutter signals are simply pieces of the clutter signal defined over time intervals of τ_p. The leading edge of the μth segmented clutter signal is located at the time

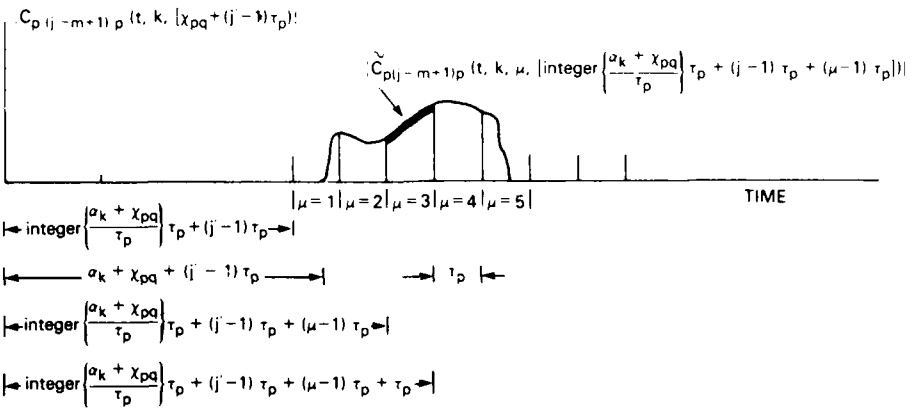

Fig. 18 — The μth segmented clutter signal

$$\text{integer}\left\{\frac{\alpha_k + \chi_{pq}}{\tau_p}\right\}\tau_p + (j'-1)\tau_p + (\mu-1)\tau_p,$$

and the trailing edge of the μth segmented clutter signal is located at the time

$$\text{integer}\left\{\frac{\alpha_k + \chi_{pq}}{\tau_p}\right\} + (j'-1)\tau_p + (\mu-1)\tau_p + \tau_p.$$

Eclipsing Conditions

High-power pulsed monostatic radars blank their receivers while they transmit. If an echo is entering the radar antenna and receiver during this time, it is not received and eclipsing is said to occur. Figure 19 illustrates the eclipsing of an echoes from a single target due to a pulse train of three pulses. The transmitted pulses are labeled $\delta(t)$, and the echoes at the input to the receiver are labeled $X(t)$. Since $\delta(t)$ is a pulse train which uses pulse modulations such as linear FM for pulse compression, only the envelope of $\delta(t)$ and of $X(t)$ is shown. These waveforms illustrate the relative timing. As Fig. 19 shows, the echoes from the first and second pulses occur during the transmission time of the second and third pulses respectively, and a partial eclipsing occurs. After the echoes are passed through the receiver and matched filter, the echoes partially eclipsed will not be completely matched to the filter. However, the last echo not eclipsed is completely matched to the filter and yields the normal desired response.

For waveforms which meet the time orthogonality condition, a few eclipsing properties can easily be computed and are shown in Table 1. The left column shows the interval of time that the single-target echo due to the first pulse of the ith pulse train must fall within for eclipsing to occur. Next the number of times the echoes are or are not eclipsed is given. The fraction of the echo eclipsed for those echoes being eclipsed is next given. Finally the number of times the filter can obtain a steady-state condition for a single target without using eclipsed or partially eclipsed echoes is computed (the number of times echoes are not eclipsed plus one minus the order of the filter M) and is shown in the table. If the quantity is negative, the quantity is set to zero. The proof of the results in Table 1 is given in Appendix A. Even if some echoes are eclipsed, the filter can reach steady-state operation and the target and clutter can be separated if they have different Doppler properties. We will not discuss the properties of waveforms which do not meet the time orthogonality condition. These properties are much more complex, because transmitted pulses from multiple pulse trains can eclipse target echoes from the ith pulse train. However, the analysis is similar.

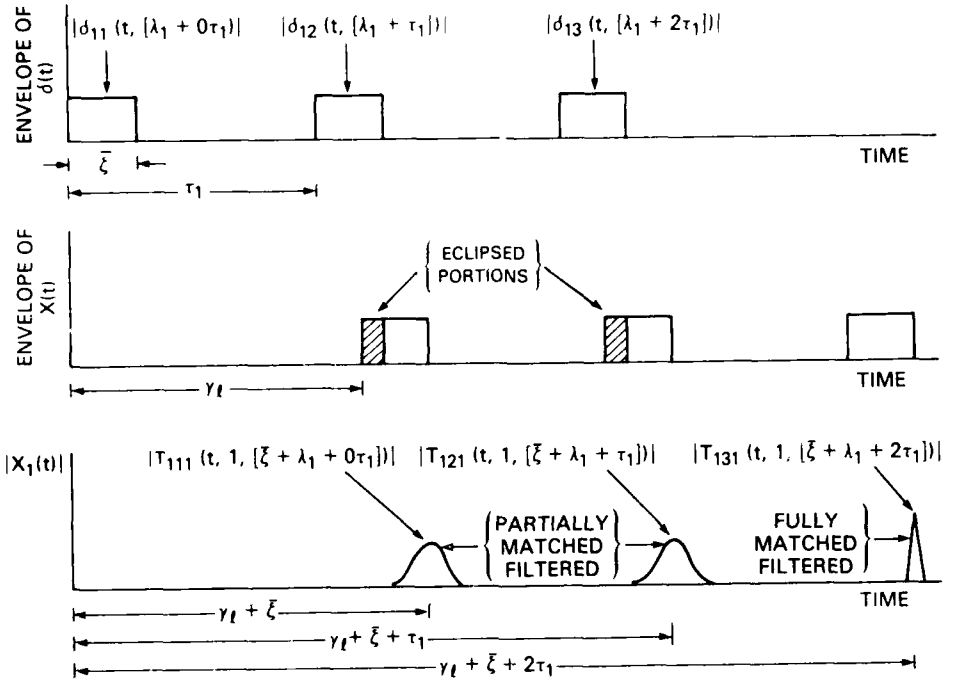

Fig. 19 — Target eclipsing for $N = 1$, $\bar{N} = 3$, $\bar{\zeta} \neq \zeta$, and a single target

Table 1 — Single-Target Eclipsing Conditions for Target Echoes Due to the ith Pulses Train Being Eclipsed by Pulses From the kth Pulse Train

Time Interval of the First Target Echo γ_l	Number of Times Echoes are		Fraction of the Time an Unprocessed Echo is Eclipsed	Number of Times the Filter Can Obtain a Steady-State Condition For a Single Target Without Using Eclipsed Echoes						
				Filter Order M =						
	Eclipsed	Not Eclipsed		2	3	4	...	$\bar{N}-2$	$\bar{N}-1$	$\bar{N}$
$0 \rightarrow \bar{\zeta}_i$	$\bar{N}$	0	$\gamma_l/\bar{\zeta}_i$	0	0	0	...	0	0	0
$\tau_i \rightarrow \tau_i + \bar{\zeta}_i$	$\bar{N}-1$	1	$\lvert\gamma_l - \tau_i\rvert/\bar{\zeta}_i$	0	0	0	...	0	0	0
$2\tau_i \rightarrow 2\tau_i + \bar{\zeta}_i$	$\bar{N}-2$	2	$\lvert\gamma_l - 2\tau_i\rvert/\bar{\zeta}_i$	1	0	0	...	0	0	0
$3\tau_i \rightarrow 3\tau_i + \zeta_i$	$\bar{N}-3$	3	$\lvert\gamma_l - 3\tau_i\rvert/\bar{\zeta}_i$	2	1	0	...	0	0	0
$4\tau_i \rightarrow 4\tau_i + \bar{\zeta}_i$	$\bar{N}-4$	4	$\lvert\gamma_l - 4\tau_i\rvert/\bar{\zeta}_i$	3	2	1	...	0	0	0
...	...	...	...	...	...	...	...	...	...	...
$(\bar{N}-2)\tau_i \rightarrow (\bar{N}-2)\tau_i + \bar{\zeta}_i$	2	$\bar{N}-2$	$\lvert\gamma_l - (\bar{N}-2)\tau_i\rvert/\bar{\zeta}_i$	$(\bar{N}-3)$	$(\bar{N}-4)$	$(\bar{N}-5)$	...	1	0	0
$(\bar{N}-1)\tau_i \rightarrow (\bar{N}-1)\tau_i + \bar{\zeta}_i$	1	$\bar{N}-1$	$\lvert\gamma_l - (\bar{N}-1)\tau_i\rvert/\bar{\zeta}_i$	$(\bar{N}-2)$	$(\bar{N}-3)$	$(\bar{N}-4)$	...	2	1	0
$\bar{N}\tau_i \rightarrow \bar{N}\tau_i + \bar{\zeta}_i$	0	$\bar{N}$	0	$(\bar{N}-1)$	$(\bar{N}-2)$	$(\bar{N}-3)$	...	3	2	1

Table 1 can also be used to describe eclipsing of clutter echoes as long as the interpretation is modified slightly. If the clutter patch extent is smaller than the time between pulses $\beta_k - \alpha_k < \tau_i$, Table 1 can be used directly with several slight modifications. The left-hand column is read as the time interval within which any part of the first clutter echo lies. The column on the fraction of time an uncompressed echo is eclipsed is not meaningful. However, the time interval the processed clutter echoes are modified due to eclipsing is bounded by $2\bar{\zeta}_i$ but may be less, depending on α_k and β_k.

When the clutter patch extent is greater than the time between pulses $\beta_k - \alpha_k > \tau_i$, the amount of eclipsing is different for different time intervals of the clutter patch. This is illustrated in Fig. 20. Since the signal $X_1(t)$ is composed of the superposition of the clutter echoes that overlap in time, the results are better illustrated by showing the magnitude of the components of $X_1(t)$. Figure 20 shows that the eclipsing affects the early part of the clutter patch three times and affects the later part of clutter patch occurring time τ_i later only two times. Using this example as a guide, the properties listed in Table 1 can be used for this case as well with the following change in interpretation. Since in these cases the clutter echo due to the first pulses can now fall into several time intervals in the left column, the properties for each clutter segment over these time intervals can be read in the right-hand columns. Consequently the filter can reach steady-state conditions for some segments of the clutter patch and not for others without using signals modified by eclipsing.

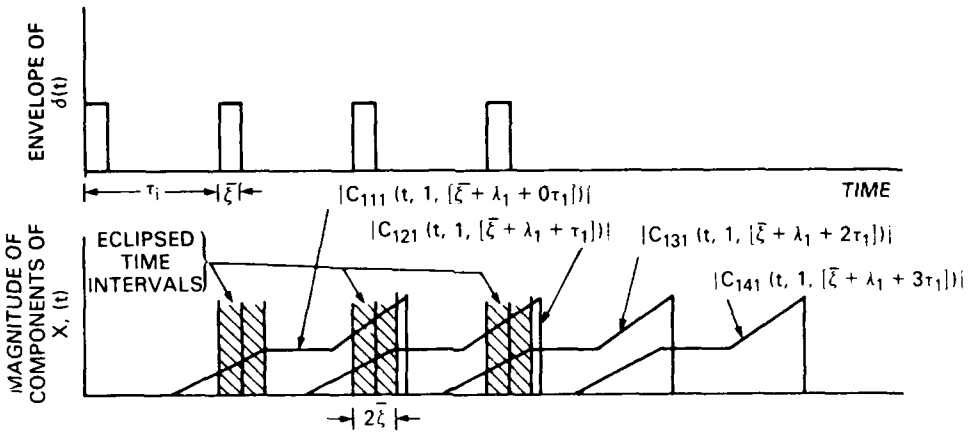

Fig. 20 — Clutter eclipsing for $N = 1$, $\bar{N} = 4$, $\bar{\zeta} \neq \zeta$, and a clutter extent that is $\beta_1 - \alpha_1 > \tau_i$

PULSE-DOPPLER AND MTI OPERATION

Most radars using Doppler processing adjust their operation to a steady state such that targets can be separated from clutter. However, often this is done without regard to the sizes and distribution of clutter patches. Consequently pulse-Doppler radars use enough pulses so that a steady-state condition is reached with respect to all clutter and targets. We will define conventional pulse-Doppler and MTI operation which is consistent with past usage but in terms of our new development.

Pulse-Doppler and MTI Definitions

Before giving the conditions for pulse-Doppler operation, the following definitions are first given. The pulse-Doppler separation time interval for clutter on the pth pulse train is defined by

$$\bar{\Delta}_p^c = \bigcap_{k=1}^{N_c} \Delta_{kp}^c,$$

and the pulse-Doppler separation time interval for targets on the pth pulse train is defined by

$$\bar{\Delta}_p^T = \bigcap_{i=1}^{N_t} \Delta_{ip}^T,$$

where $\cap$ is the symbol for intersection. These separation time intervals are simply the smallest time interval contained in all the clutter or target separation time intervals respectively. The pulse-Doppler separation time interval for clutter is illustrated in Fig. 21. The condition for pulse-Doppler operation can then be stated as follows.

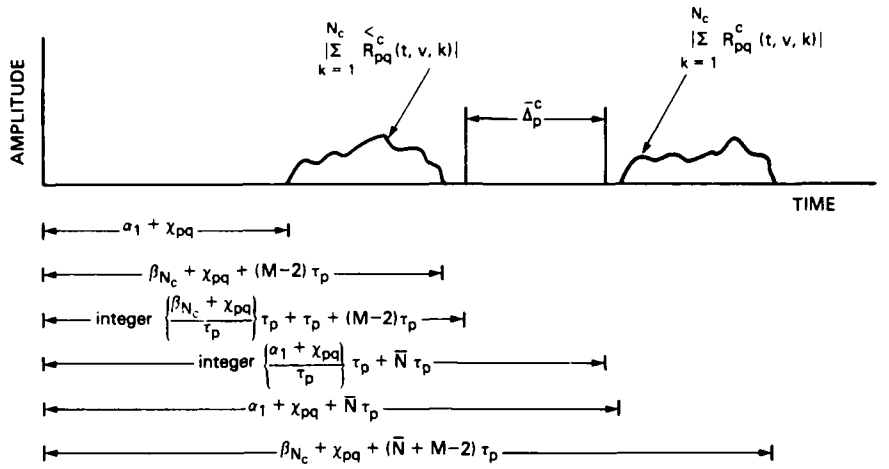

Fig. 21 — Pulse-Doppler separation time interval for clutter for the pth pulse train which meets the pulse-Doppler operation condition ($\bar{\Delta}_p^c > \tau_p$)

Definition of the Condition for Conventional Pulse-Doppler and MTI Operation. For pulse trains which meet the time orthogonality or frequency orthogonality condition, the condition for pulse-Doppler or MTI operation on the $i = p$th pulse train requires that the intersection of the pulse-Doppler separation time intervals for clutter $\bar{\Delta}_p^c$ and targets $\bar{\Delta}_p^T$ on the pth pulse train be greater than the pulse-repetition interval τ_p in width. This is written as

$$\text{width of } \{\bar{\Delta}_p^c \cap \bar{\Delta}_p^T\} > \tau_p.$$

Furthermore, if the condition

$$1 > \max \begin{Bmatrix} (\beta_{N_c} + \chi_{pq})/\tau_p \\ \text{or} \\ (\gamma_{N_t} + \chi_{pq} + \bar{\zeta}_i)/\tau_p \end{Bmatrix} - \min \begin{Bmatrix} (\alpha_1 + \chi_{pq})/\tau_p \\ \text{or} \\ (\gamma_1 + \chi_{pq} - \bar{\zeta}_i)/\tau_p \end{Bmatrix}$$

is met, where $\max \begin{Bmatrix} (\beta_{N_c} + \chi_{pq}) \\ \text{or} \\ (\gamma_{N_t} + \chi_{pq} + \bar{\zeta}_i) \end{Bmatrix}$ is the farthest radar echo and $\min \begin{Bmatrix} (\alpha_1 + \chi_{pq}) \\ \text{or} \\ (\gamma_1 + \chi_{pq} - \bar{\zeta}_i) \end{Bmatrix}$ is the nearest radar echo, then the condition stated is for MTI operation (unambiguous range), otherwise it is for pulse-Doppler operation.

This definition is a condition on the global requirements for steady-state operation of the filter. The filter is in steady-state operation with respect to all echoes due to the $(i = p)$th pulse train for at least one pulse-repetition interval. Consequently, if the clutter and targets have significantly different Doppler shifts and the pulse-repetition interval is short enough, the targets can be separated from the clutter with the filter over the time frame that the global steady-state condition exists. Furthermore,

the targets will appear at least once over the time frame $\bar{\Delta}_p^c \cap \bar{\Delta}_p^T$, since this time frame is greater than τ_p and target echoes appear at time intervals of τ_p when the filter is in steady-state operation.

The second requirement defines the operation as MTI or pulse Doppler along conventional lines. For MTI operation, the range is unambiguous, and consequently the pulse-repetition interval exceeds the distance between the furthest and nearest echo measured in time. Otherwise, the range is ambiguous, and the operation is defined as being pulse Doppler. We next investigate requirements for and properties of the pulse-Doppler and MTI operation.

Requirement on Transmitted Pulses

For the filter to reach steady-state operation and the conditions for pulse-Doppler operation to be met, a number of pulses must be transmitted. The requirement on the number of pulses needed is stated in the following theorem.

Theorem on the Number of Pulses Required for Pulse-Doppler and MTI Operation: If a pulse train meets the condition for pulse-Doppler or MTI operation, the number of transmitted pulses on the ith pulse train $\bar{N}$ must be

$$\bar{N} \geqslant \text{integer}\left[\max\begin{Bmatrix}(\beta_{N_c} + \chi_{pq})/\tau_p \\ \text{or} \\ (\gamma_{N_t} + \chi_{pq} + \bar{\zeta}_i)/\tau_p\end{Bmatrix}\right] - \text{integer}\left[\min\begin{Bmatrix}(\alpha_1 + \chi_{pq})/\tau_p \\ \text{or} \\ (\gamma_1 + \chi_{pq} + \bar{\zeta}_i)/\tau_p\end{Bmatrix}\right] + M$$

for pulse-Doppler operation. For the special case of MTI operation

$$\bar{N} \geqslant M \text{ or } \bar{N} \geqslant M + 1,$$

depending on the relative values of the nearest and farthest echoes to the time intervals τ_p measured from time equal to zero.

The proof of the theorem is given in Appendix B. This theorem basically states that the number of pulses required for pulse-Doppler operation is enough to fill the filter of order M plus the number of puises required to extend from the nearest echo to the farthest echo. This further means a need to keep transmitting in the presence of nearby targets until the farthest echo is received and the filter is filled so steady-state conditions are met.

Pulse-Doppler Clutter Stacking Theorem

A well-known property of pulse-Doppler radars is that the clutter echoes are superimposed from all ranges which are a multiple of the range equivalent of the pulse-repetition interval and that the echoes anywhere in range are not superimposed for MTI operation. We restate this property as a theorem and prove it in Appendix B in terms of our previous mathematical structure.

Pulse-Doppler Clutter Stacking Theorem. At any instant of time, over the pulse-Doppler separation time intervals for clutter and targets for the pth pulse train, the filter response is due to the excitation formed from the superposition of echoes from the pth pulse train belonging to each clutter patch segment $\mu = 1, 2, \ldots, N_k$ of each clutter patch for $k = 1, 2, \ldots, N_c$. Furthermore, if the MTI condition is met, the filtered steady-state echoes of $S_{pq}^c(t, \mathrm{v}, k)$ at any instant of time is due to one and only one clutter-patch segment of one and only one clutter patch.

A Counting Theorem

It is useful to know the number of times a target will appear in the pulse-Doppler separation time interval. This result is stated as a theorem, and the proof is given in Appendix B.

Counting Theorem. The number N_S of target separation signals $S_{pq}^{T}(t, v, l)$, for the lth target due to the pth pulse train which meets the condition for pulse-Doppler operation that appears in the pulse-Doppler separation time interval is given by

$$N_S = \text{integer}\left[\min\begin{Bmatrix}(\alpha_1 + \chi_{pq})/\tau_p \\ \text{or} \\ (\gamma_1 + \chi_{pq} - \bar{\zeta}_l)/\tau_p\end{Bmatrix}\right] - \text{integer}\left[\max\begin{Bmatrix}(\beta_{N_t} + \chi_{pq})/\tau_p \\ \text{or} \\ (\gamma_1 + \chi_{pq} + \bar{\zeta}_l)/\tau_p\end{Bmatrix}\right] + (\bar{N} - M + 1).$$

Range Ambiguities

A well-known property of pulse-Doppler radars is that range is ambiguous. This will be stated as a theorem. No proof of this will be given, since it is well known. Interpreting the property in our notation, we note that the filter is in steady-state operation with respect to all echoes over the pulse-Doppler separation time interval. Then all targets that are multiples of the pulse-repetition interval are located in the same place in range over this interval.

Theorem on Target Range Ambiguities for Pulse-Doppler Radars. For a pulse train which meets the pulse-Doppler condition, all targets separated by multiples of the pulse-repetition interval τ_p will be ambiguous in range.

CONTROLLED-PULSE-DOPPLER OPERATION

The previously described material has set the stage for properly presenting the main developments of this study, which are described next. We will show that the filter can obtain steady-state operation with respect to echoes from a given clutter patch and will show that over the time interval in which this occurs no other signals due to other clutter patches are present. Consequently the targets can be separated from the clutter in each clutter patch individually. However, certain conditions must be met and the results must be properly interpreted before this operation can be achieved.

Definition of Controlled-Pulse-Doppler Operation

We begin the development by defining the requirements for obtaining pulse-Doppler operation on a clutter patch.

Definition of the Condition for Controlled-Pulse-Doppler (CPD) Operation. For pulse trains which meet the time orthogonality or frequency orthogonality condition, the condition for CPD operation on the kth clutter patch and the $(i = p)$th pulse train requires that the width of the separation time interval for the kth clutter patch and pth pulse train Δ_{kp}^{ξ} be greater than τ_p, which is written as: width of $\Delta_{kp}^{\xi} > \tau_p$. Furthermore over Δ_{kp}^{ξ} we require that there be no other signals present due to other clutter patches. Finally, if the condition

$$\beta_k - \alpha_k < \tau_p$$

is met, we say the operation is controlled MTI (CMTI) operation (unambiguous range across the clutter patch), otherwise we say it is CPD operation.

This definition is a condition on the local requirements for steady-state operation of the filter. Consequently, if the kth clutter patch and targets contained within it have significantly different Doppler shifts and the pulse repetition interval is short enough, targets can be separated from the kth clutter patch with the filter over the time frame that the local steady-state conditions exists. Furthermore, the targets will appear at least once over the time frame of Δ_{kp}^{ξ}, since this time frame is greater than τ_p and target echoes appear at time intervals τ_p when the filter is in steady-state operation. The

second requirement defines the operation as MTI or pulse Doppler with respect to a particular clutter patch. For MTI clutter-patch operation the range is unambiguous across the clutter patch. Otherwise, the range is ambiguous across the clutter patch, and the operation is defined as being pulse Doppler. We next investigate requirements for and properties of the CPD operation.

Requirement on Transmitted Pulses

For the filter to reach steady-state operations with respect to a particular clutter patch so that one of the conditions for CPD operation is met, the number of transmitted pulses must meet a requirement. This requirement is stated in the following theorem, which is proved in Appendix C.

Theorem on the Number of Pulses Required for CPD Operation. If a pulse train meets the condition for CPD operation on the kth clutter patch, the number of transmitted pulses on the ith pulse train $\bar{N}$ must be

$$\bar{N} \geqslant \text{integer}\,\{(\beta_k + \chi_{pq})/\tau_p\} - \text{integer}\{(\alpha_k + \chi_{pq})/\tau_p\} + M$$

for CPD operation. For the special case of CMTI operation

$$\bar{N} \geqslant M \text{ or } \bar{N} \geqslant M + 1,$$

depending on the relative values of the leading and trailing edge of the clutter patch with respect to the time intervals τ_p measured from time equal to zero.

Controlled-Pulse-Doppler Clutter Stacking Theorem

For CPD operation, in a similar manner as we described for pulse-Doppler radars, clutter echoes are superimposed from ranges which are multiples of the range equivalent of the pulse-repetition interval. However, the clutter echoes are stacked from only a portion of the ranges, because of the short duration of the pulse train. We state the property in a theorem.

CPD Clutter Stacking Theorem. At any instant of time over the separation time interval for the kth clutter patch and the pth pulse train Δ_{pk}^{c}, the filter response is due to the superposition of echoes belonging to all the kth clutter-patch segments $\mu = 1, 2, \ldots, N_k$ but no other clutter echoes under the CPD operating conditions. Furthermore, if the CMTI condition is met, the filter response under these conditions is due to one and only one clutter-patch segment.

The proof has already been given as a portion of the proof of the pulse-Doppler clutter stacking theorem in Appendix B. In that theorem it was necessary to show the clutter stacking results individually before the collective results were given.

A Counting Theorem

It is useful to know the number of times a target will appear in the separation time interval, and the result is stated as the following theorem, which is proved in Appendix C.

CPD Counting Theorem. The number $N_s(k)$ of target separation signals $S_{pq}^{T}(t, \text{v}, l)$ that appears in the separation time interval Δ_{kp}^{c} for the lth target located in the kth clutter patch and due to the pth pulse train which meets the CPD condition is given by

$$N_s(k) = \text{integer}\,[(\alpha_k + \chi_{pq})/\tau_p] - \text{integer}\,[(\beta_k + \chi_{pq})/\tau_p] + \bar{N} - M + 1.$$

Separation Requirements

We have investigated the requirements for unmasking a target in the kth clutter patch. We next investigate the requirements for not corrupting this result with echoes from other clutter patches. The

conditions we need are illustrated in Fig. 22. The transient decay of the $(k-1)$th filter given by the right remainder signal $\overset{>}{R}{}^{c}_{pq}(t, v, k-1)$ must end before the kth-clutter-patch separation time interval Δ^{c}_{kp} begins. Furthermore Δ^{c}_{kp} must end before the transient buildup of the filter begins for the $(k+1)$th clutter patch. The conditions which must be met to ensure this operation is stated in the following theorem and proved in Appendix C.

Theorem on CPD Separation Requirement 1. For a pulse train to meet the CPD requirements, the leading edge of the $(k+1)$th clutter patch α_{k+1} must be a distance of

$$\alpha_{k+1} \geqslant \text{integer}\,\{(\beta_k + \chi_{pq}/\tau_p)\}\tau_p - \chi_{pq} + (N_s(k) + M - 1)\tau_p$$

from the kth clutter patch, and the kth clutter patch must be a distance of

$$\text{integer}\,\{(\alpha_k + \chi_{pq})/\tau_p)\}\tau_p - \chi_{pq} \geqslant \beta_{k-1} + (N_s(k) + M - 2)\tau_p$$

from the $(k-1)$th clutter patch.

This theorem is important, because it shows that the number of pulses $\bar{N}$ and pulse spacing τ_p must be chosen such that a separation time interval is obtained and is not corrupted with echoes from other clutter patches. The requirements are illustrated in Fig. 23. The figure shows that for small $N_s(k)$ and M the clutter-patch separations equal just several pulse-repetition intervals τ_p. Consequently for short values of τ_p the patches can be fairly closely spaced and yet the CPD operation can be obtained.

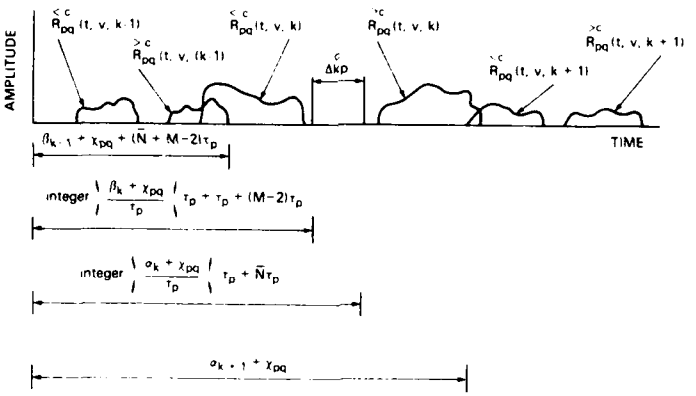

Fig. 22 — Conditions necessary to keep other-clutter-patch echoes from corrupting the βth clutter patch

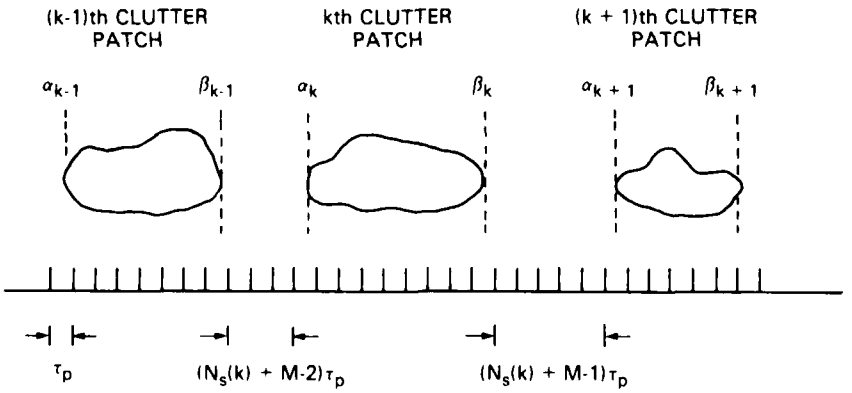

Fig. 23 — Clutter patch separation for CPD operation

The next question that arises is whether one unmasks targets in other clutter patches when one is set up to extract targets from say the $(k = k^*)$th patch. The situation is illustrated in Fig. 24, which shows that there are a number of intervals of length τ_p across the separation time interval $\Delta_{kp}^{\cdot}$ because the range extent of the k^*th patch exceeds the range extent kth patch. These intervals are labeled $s = 1, 2, \ldots, N_s(k)$. We require one of these intervals $s = s^*$ to not be covered by remainder signals from adjacent clutter patches. From these thoughts a requirement on the closeness of adjacent clutter patches can be obtained, expressed in the following theorem.

Theorem on CPD Separation Requirement 2. **Given a pulse train that meets the CPD requirements for the k^*th clutter patch, it is possible to obtain steady-state operation for the kth patch over at least one time interval τ_p and not be covered by remainder signals from itself or other clutter patches if the following requirements are met:**

- $(\beta_{k^*} - \alpha_{k^*}) > (\beta_k - \alpha_k)$,
- there is a value s in which both

$$\text{integer}\{(\alpha_k + \chi_{pq})/\tau_p\}\,\tau_p > (\beta_{k-1} + \chi_{pq}) + (M-2)\tau_p + (N_s(k) - s)\tau_p$$

and

$$\alpha_{k+1} > \text{integer}\{(\beta_k + \chi_{pq})/\tau_p\}\,\tau_p + \tau_p + (M-2)\tau_p + (s+1)\tau_p - \chi_{pq}$$

are true and s can vary from 1 to $N_s(k)$.

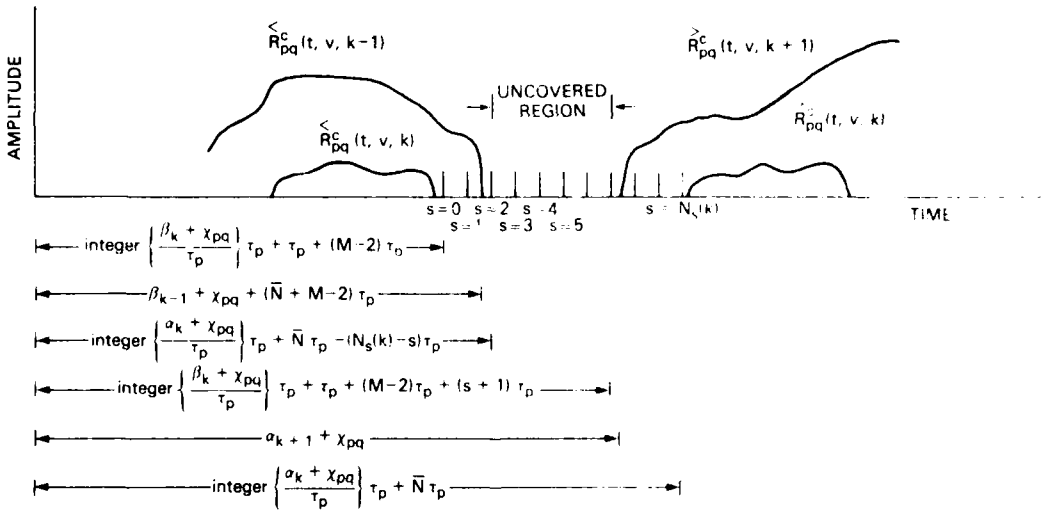

Fig. 24 — Remainder signals and the separation time interval for the kth clutter patch when the number of pulses is set by the k^*th clutter patch

The theorem basically states that for those patches of less range extent than the range extent of the k^*th patch one can extract targets if the distance between the nearest edges of the adjacent patches is greater than an integer multiple of the pulse-repetition interval τ_p, as illustrated in Fig. 25. Using this theorem and the others concerning CPD we are now in a position to discuss how an algorithm for choosing the pulse burst could be designed.

We could start the algorithm by finding the patch with the longest range extent and determine the pulse-repetition interval τ_p and number of pulses $\bar{N}$ in the pulse train to obtain CPD operation for this patch. Next we could determine if targets in other clutter patches can be found by using the results of

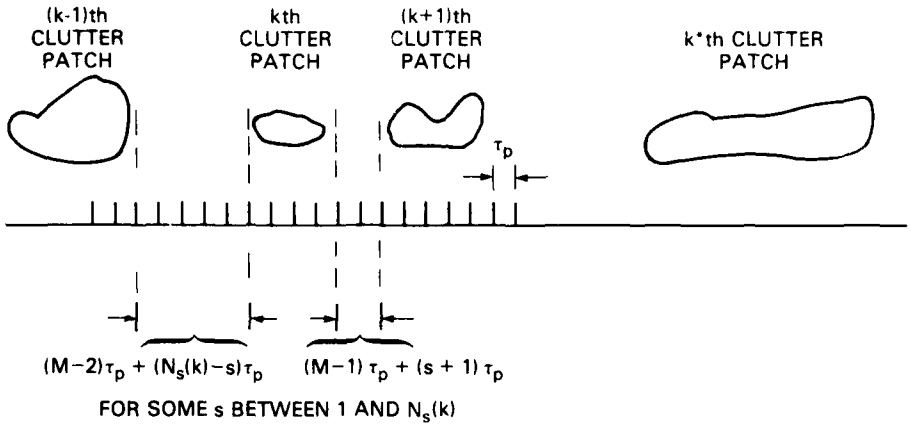

Fig. 25 — Spacial separation requirements to see targets in other patches when CPD-operation conditions are set on the k^* patch

the theorem on CPD separation requirement 2. If all these conditions are satisfied, the one pulse burst will unmask all targets in all patches. If the conditions are not satisfied, we have three fundamental choices: use more than one burst, redefine patches by combining some into a single patch, or not see in all patches. The algorithm must incorporate judgment then as to what is most important before the pulse bursts are determined. Some examples of what the algorithm might do is as follows. Two small closely spaced patches might be combined into a single patch so that all requirements are met. Possibly one large patch is far out in range and several smaller chaff patches are up close. The operation could be set nominally so that every observation would look in the several smaller chaff patches and every fourth observation would look in the patch out in range. The design of this algorithm is beyond the scope of this development, which is concerned with fundamentals of the processes and detailed implementations.

Range Ambiguities

The CPD operation has target range ambiguities like those of the conventional pulse-Doppler systems. However, the pulse train that meets CPD requirements consists of only a short burst of pulses, and there are much fewer ambiguities. The following theorem gives the interval where the target range is ambiguous and a formula for computing the number of possible range ambiguities for targets detected in the kth clutter patch. The proof is given in Appendix C.

Theorem on Target Range Ambiguities for CPD Operation. For a pulse train that meets the CPD condition for the kth clutter patch, targets separated by multiplies of the pulse-repetition interval τ_p and located in the interval γ_l such that

$$\gamma_l < \text{integer}\{(\alpha_k + \chi_{pq})/\tau_p\} - \chi_{pq} - (M-2)\tau_p$$

and

$$\gamma_l > \text{integer}\{(\beta_k + \chi_{pq}/\tau_p\} - \chi_{pq} + (M-1)\tau_p$$

will be ambiguous in range. The number of range ambiguities is given by

$$\text{integer}\{(\beta_k + \chi_{pq})/\tau_p\} - \text{integer}\{(\alpha_k + \chi_{pq})/\tau_p\} + 2M - 3.$$

Example of Performance

We will compare the performance of an ordinary pulse-Doppler radar and one using a short pulse burst which is configured to see in a clutter patch. The geometry is shown in Fig. 26. A shipboard S-band radar (wavelength $\lambda = 10$ cm) illuminates the sea close in range and a heavy wind-blown rain

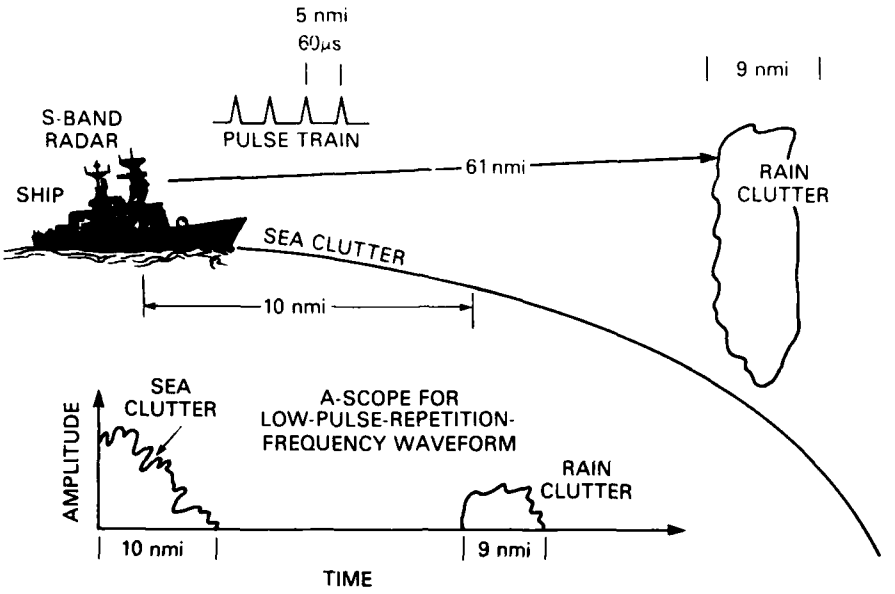

Fig. 26 — Echo geometry

cloud between 61 and 70 nmi away. The time between pulses τ_p is 60 μs, which corresponds to 5 nmi unambiguous range. A target is located at 62 nmi. Consequently a conventional pulse-Doppler radar will receive simultaneously sea-clutter echoes from 2 and 7 nmi, rain-clutter echoes from 62 and 67 nmi, and the target echo. The cross section of these clutter echoes are shown in Table 2.

We will use a three-pulse canceler for both the pulse-Doppler and CPD cases. The formula for computing the cancellation ratio is given on page 219 of Ref. 3:

$$C = \sqrt{3}\left[\frac{4\pi\tau_p\sigma_v}{\lambda}\right]^2,$$

where σ_v is the clutter spread. Using a σ_v of 1 m/s for sea clutter and a σ_v of 6 m/s for rain clutter, we obtain cancellation ratios of −79 dB and −48 dB respectively. However, we assume the equipment limits the cancellation to −45 dB, which is the limiting factor. Table 2 shows the cross sections after cancellation.

Table 2 — Clutter Cross Sections at Selected Ranges Before and After Clutter Processing*

Type of Clutter Patch	Selected Range for Computing the Clutter Cross Section (nmi)	Clutter Cross Section* (dB re 1 m^2)	
		Before Cancellation	After Cancellation
Sea clutter	2	−2	−45
	7	−7	−52
Rain clutter	62	+26	−19
	67	+26	−19

*The parameters used in computing the cross section were as follows: azimuth bandwidth = 2°, pulse width = 300 m, antenna height = 30 m, sea state = 4, backscatter coefficient = −48 dB at 2 nmi and −58 dB at 7 nmi, rain-cloud height = 6 km, rainfall rate = 16 mm/h, and backscatter coefficient = −73 dB.

We next compute the number of pulses in a pulse train required for the CPD radar to see a target in the rain cloud using

$$\bar{N} \geqslant \text{integer}\{(\beta_k + \chi_{pq})/\tau_p\} - \text{integer}\{(\alpha_k + \chi_{pq})/\tau_p\} + M,$$

where

$$\chi_{pq} = \bar{\zeta} + \lambda_N + (\bar{N} + M - 2)\,\bar{\tau}_i - (q-1)\tau_p,$$

and noting that $\bar{\zeta} = 1\ \mu s$, $\lambda_N = 0$, $\alpha_1 = 0$, $\beta_1 = 120\ \mu s$, $\tau_1 = 60\ \mu s$, $\tau = 60\ \mu s$, $\alpha_2 = 732\ \mu s$, $\beta_2 = 840\ \mu s$, $N_i = 1$, $M = 3$, $N_k = 1$, and $N_v = 1$.

Solving for $\bar{N}$ iteratively, we find $\bar{N} = 5$ will satisfy the requirements for CPD operation. Under this condition $N_s(k) = 1$, which implies that a target in the rain cloud will appear one time in separation time interval Δf_1 for CPD operation. We next compute to see if the two clutter patches are separated enough by

$$\text{integer}\{(\alpha_2 + \chi_{pq})/\tau_1\}\,\tau_1 + \chi_{pq} \geqslant \beta_1 + (N_s(k) + M - 2)\tau_p$$

for CPD operation. We find this inequality to be true.

We can now compare pulse-Doppler and CPD operation. The CPD-operation performance is obtained directly by noting that the cancellation in both patches are independent. Consequently from Table 2 we find that the clutter cross section after cancellation of the rain clutter is $-19 + 3$ dB $= -16$ dB re 1 m^2. The 3-dB increase in clutter cross section is due to stacking of the two clutter segments in the rain cloud. Consequently under clutter-limited conditions a 42-dB improvement in signal-to-clutter ratio has been obtained on the target located at 62 nmi in the heavy wind-blown rain cloud. A target with a cross section of about 0.5 m^2 can then be detected in the rain cloud.

We next compute the performance of the pulse-Doppler operation. In this case the clutter from ranges of 2, 7, 62, and 72 nmi are stacked on top of each other. By far the strongest echo is the one at 2 nmi because of its short range. We compute its equivalent cross section as if it would have been at 62 nmi by

$$\text{cross section at 62 nmi} = (\text{cross section at 2 nmi}) \left(\frac{62}{2}\right)^4.$$

Since the cross section at 2 nmi is -47 dB re 1 m^2, after cancellation its equivalent cross section at 62 nmi (the same as the target) is $+2$ dB re 1 m^2. Consequently the clutter cross section after cancellation for the pulse-Doppler operation is 18 dB worse than for the CPD operation, and now a target of 15 dB re 1 m^2 would be required for detection. Furthermore only five range ambiguities need to be resolved for the CPD operation versus approximately 40 for the 200-nmi-maximum-range pulse-Doppler radar.

SUMMARY

The Doppler processing of radar echoes was studied under the condition that the location and range extents of the clutter patches was known or measured. A mathematical structure was developed to describe the processes, and conventional pulse-Doppler and MTI operations were reviewed within this structure. We showed that pulse-Doppler and MTI systems obtained a global steady-state operation with respect to all clutter. However, we showed that it was possible to obtain a local steady-state Doppler processing operation with respect to each clutter patch individually (controlled-pulse-Doppler, or CPD operation) if certain conditions were met. Basically the pulse-repetition interval and the number of pulses transmitted must be set based on the clutter environment consisting of range extents of the clutter patches and decorrelation time of the clutter.

The general result is that, if the clutter is patchy, targets and clutter can be separated in each clutter patch individually by use of short pulse bursts. Under these conditions, there are often few range ambiguities to resolve, there is little stacking of clutter residues, and there often is no eclipsing except possibly at short range. These results and the fact that short pulse-repetition intervals can be used to keep the clutter correlated show that the CPD operation can yield significantly improved performance over conventional pulse-Doppler and MTI systems. A simple example was shown to illustrate this fact.

REFERENCES

1. M.I. Skolnik, *Introduction to Radar Systems,* McGraw-Hill, New York, 1962.

2. N.R. Gillespie, J.B. Higley, and N. MacKinnon, "The Evolution and Application of Coherent Radar Systems," IRE Transactions on Military Electronics, **MIL-5** (No. 2), 131-139 (Apr. 1961).

3. D. Barton, *Radar System Analysis,* Prentice-Hall, Englewood Cliffs, N.J., 1964.

4. F. Nathanson, *Radar Signal Processing and the Environment,* McGraw-Hill, New York, 1969.

5. M.I. Skolnik, editor, *Radar Handbook,* McGraw-Hill, New York, 1970.

Appendix A
PROOFS OF BASIC THEOREMS

PROOF OF LEMMA 1

We restate Lemma 1 and prove it.

Lemma 1: The time orthogonality condition is met if

$$(\lambda_{i+1} - \lambda_i) > (\bar{N} - 1)\tau_i + \max\begin{Bmatrix}\beta_{N_c}\\ \gamma_{N_t}\end{Bmatrix} - \min\begin{Bmatrix}\alpha_1\\ \gamma_1\end{Bmatrix}, \quad \text{for all } i.$$

Proof: if $p > i$, the last echo in $\hat{Z}_{pq}(t, \mathrm{v})$, given by

$$\bar{\zeta} + \lambda_i + (\bar{N} - 1)\tau_i + (m - 1)\tau_p + (\lambda_N - \lambda_p) + (q - 1)(\bar{\tau} - \tau_p) + (\bar{N} + m - 1 - q)\bar{\tau} + \max\begin{Bmatrix}\beta_{N_c}\\ \gamma_{N_t}\end{Bmatrix},$$

must be present before the first echo in $\tilde{Z}_{pq}(t, \mathrm{v})$, given by

$$\bar{\zeta} + \lambda_N + (\bar{N} + m - 2)\bar{\tau} + (1 + m - 2)\tau_p - (q - 1)\tau_p + \min\begin{Bmatrix}\alpha_1\\ \gamma_1\end{Bmatrix}.$$

Forming the inequality, we obtain

$$\lambda_p - \lambda_i > (\bar{N} - 1)\tau_i + \max\begin{Bmatrix}\beta_{N_c}\\ \gamma_{N_t}\end{Bmatrix} - \min\begin{Bmatrix}\alpha_1\\ \gamma_1\end{Bmatrix}.$$

Since $\lambda_p > \lambda_i$ for all $p > i$, it is then sufficient to require

$$\lambda_{i+1} - \lambda_i > (\bar{N} - 1)\tau_i + \max\begin{Bmatrix}\beta_{N_c}\\ \gamma_{N_t}\end{Bmatrix} - \min\begin{Bmatrix}\alpha_1\\ \gamma_1\end{Bmatrix}$$

for all i.

Furthermore, if $p < i$, the first echo in $\hat{Z}_{pq}(t, \mathrm{v})$, given by

$$\bar{\zeta} + \lambda_i + 0\tau_i + (m - 1)\tau_p + (\lambda_N - \lambda_p) + (q - 1)(\bar{\tau} - \tau_p) + (\bar{N} + M - 2)\bar{\tau} - (q - 1)\bar{\tau} + \min\begin{Bmatrix}\alpha_1\\ \gamma_1\end{Bmatrix},$$

must occur after the last echo in $\tilde{Z}_{pq}(t, \mathrm{v})$, given by

$$\bar{\zeta} + \lambda_N + (\bar{N} + M - 2)\bar{\tau} + (\bar{N} - 1)\tau_p + (M - 1)\tau_p - (q - 1)\tau_p + \max\begin{Bmatrix}\beta_{N_c}\\ \gamma_{N_t}\end{Bmatrix}.$$

Forming the inequality, we obtain

$$\lambda_i - \lambda_p > (\bar{N} - 1)\tau_p + \max\begin{Bmatrix}\beta_{N_c}\\ \gamma_{N_t}\end{Bmatrix} - \min\begin{Bmatrix}\alpha_1\\ \gamma_1\end{Bmatrix}.$$

Since $\lambda_i > \lambda_p$ for $i > p$, then

$$\lambda_{i+1} - \lambda_i > (\bar{N} - 1)\tau_p + \max\begin{Bmatrix}\beta_{N_c}\\ \gamma_{N_t}\end{Bmatrix} - \min\begin{Bmatrix}\alpha_1\\ \gamma_1\end{Bmatrix}.$$

The same result is obtained for $i < p$ and for $i > p$.

Q.E.D

PROOF OF THE REARRANGEMENT THEOREM

The rearrangement theorem will be proved for only clutter, because the case for targets is analogous. The expressions for

$$\tilde{Z}^c_{pq}(t, \nu) = \sum_{k=1}^{N_c} \sum_{m=1}^{M} \sum_{j=1}^{\bar{N}} W_{p\nu m} C_{pjp}(t, k, [\bar{\zeta} + \lambda_N + (\bar{N} + M - 2)\bar{\tau} + (j + m - 2)\tau_p - (q-1)\tau_p])$$

and

$$\tilde{Z}^T_{pq}(t, \nu) = \sum_{l=1}^{N_t} \sum_{m=1}^{M} \sum_{j=1}^{\bar{N}} W_{p\nu m} T_{pjp}(t, l, [\bar{\zeta} + \lambda_N + (\bar{N} + M - 2)\bar{\tau} + (j + M - 2)\tau_p - (q-1)\tau_p])$$

are defined so that when applied to

$$\tilde{Z}_{pq}(t, \nu) = \tilde{Z}^T_{pq}(t, \nu) + \tilde{Z}^c_{pq}(t, \nu),$$

the defining equation for $\tilde{Z}_{pq}(t, \nu)$, Eq. (13), is obtained.

Furthermore we may write

$$\tilde{Z}^c_{pq}(t, \nu) = \sum_{k=1}^{N_c} \sum_{m=1}^{M} W_{p\nu m} \sum_{j=1}^{\bar{N}} C_{pjp}(t, k, [\chi_{pq} + (j + m - 2)\tau_p]),$$

where

$$\chi_{pq} = \bar{\zeta} + \lambda_N + (\bar{N} + M - 2)\bar{\tau} - (q-1)\tau_p.$$

The sum over j may next be divided into three parts:

$$\begin{aligned}\tilde{Z}^c_{pq}(t, \nu) = \sum_{k=1}^{N_c} \sum_{m=1}^{M} W_{p\nu m} \Bigg\{ & \sum_{j=1}^{M-m} C_{pjp}(t, k, [\chi_{pq} + (j + m - 2)\tau_p]) \\ & + \sum_{j=\bar{M}-m+1}^{\bar{N}-m+1} C_{pjp}(k, [\chi_{pq} + (j + m - 2)\tau_p]) \\ & + \sum_{j=\bar{N}-m+2}^{\bar{N}} C_{pjp}(k, [\chi_{pq} + (j + m - 2)\tau_p]) \Bigg\}.\end{aligned}$$

We redefine the index over j as

$$j' = j + m - 1,$$

and $\tilde{Z}^c_{pq}(t, \nu)$ becomes

$$\begin{aligned}\tilde{Z}^c_{pq}(t, \nu) = \sum_{k=1}^{N_c} \Bigg\{ & \sum_{m=1}^{M} \sum_{j'=m}^{M-1} W_{p\nu m} C_{p(j'-m+1)p}(t, k, [\chi_{pq} + (j' - 1)\tau_p]) \\ & + \sum_{m=1}^{M} \sum_{j'=M}^{\bar{N}} W_{p\nu m} C_{p(j'-m+1)p}(t, k, [\chi_{pq} + (j' - 1)\tau_p]) \\ & + \sum_{m=1}^{M} \sum_{j'=\bar{N}+1}^{\bar{N}+m-1} W_{p\nu m} C_{p(j'-m+1)p}(t, k, [\chi_{pq} + (j' - 1)\tau_p]) \Bigg\}.\end{aligned}$$

The summations over m and j' can be rewritten by interchanging the order of summations. The first case is

$$\sum_{m=1}^{M} \sum_{j'=m}^{M-1} W_{p\nu m} C_{p(j'-m+1)p}(t, k, [\chi_{pq} + (j' - 1)\tau_p]) = \sum_{j'=1}^{M-1} \sum_{m=1}^{j'} W_{p\nu m} C_{p(j'-m+1)p}(t, k, [\chi_{pq} + (j' -)\tau_p]).$$

The second case is

$$\sum_{m=1}^{M}\sum_{j'=M}^{\bar{N}} W_{pvm}C_{p(j'-m+1)p}(t,\ k,\ [\chi_{pq}+(j'-1)\tau_p]) = \sum_{j'=M}^{\bar{N}}\sum_{m=1}^{M} W_{pvm}C_{p(j'-m+1)p}(t,\ k,\ [\chi_{pq}+(j'-1)\tau_p]).$$

The third case is

$$\sum_{m=1}^{M}\sum_{j'=\bar{N}+1}^{\bar{N}+m-1} W_{pvm}C_{p(j'-m+1)p}(t,\ k,\ [\chi_{pq}+(j'-1)\tau_p]) = \sum_{j'=\bar{N}+1}^{\bar{N}+m-1}\sum_{m=j'-\bar{N}+1}^{M} W_{pvm}C_{p(j'-m+1)p}(t,\ k,\ [\chi_{pq}+(j'-1)\tau_p]).$$

Using the reversed-order summations, we can rewrite $\tilde{Z}^c_{pq}(t,\ \mathrm{v})$ as

$$\begin{aligned}\tilde{Z}^c_{pq}(t,\ \mathrm{v}) = \sum_{k=1}^{N_c}\Bigg\{ &\sum_{j'=1}^{M-1}\sum_{m=1}^{j'} W_{pvm}C_{p(j'-m+1)p}(t,\ k,\ [\chi_{pq}+(j'-1)\tau_p]) \\ &+ \sum_{j'=M}^{\bar{N}}\sum_{m=1}^{M} W_{pvm}C_{p(j'-m+1)p}(t,\ k,\ [\chi_{pq}+(j'-1)\tau_p]) \\ &+ \sum_{j'=\bar{N}+1}^{\bar{N}+M-1}\sum_{m=j'-\bar{N}+1}^{M} W_{pvm}C_{p(j'-m+1)p}(t,\ k,\ [\chi_{pq}+(j'-1)\tau_p])\Bigg\}.\end{aligned}$$

We define

$$\overset{<}{R}{}^c_{pq}(t,\ \mathrm{v},\ k) = \sum_{j'=1}^{M-1}\sum_{m=1}^{j'} W_{pvm}C_{p(j'-m+1)p}(t,\ k,\ [\chi_{pq}+(j'-1)\tau_p]),$$

$$S^c_{pq}(t,\ \mathrm{v},\ k) = \sum_{j'=M}^{\bar{N}}\sum_{m=1}^{M} W_{pvm}C_{p(j'-m+1)p}(t,\ k,\ [\chi_{pq}+(j'-1)\tau_p]),$$

$$\overset{>}{R}{}^c_{pq}(t,\ \mathrm{v},\ k) = \sum_{j'=\bar{N}+1}^{\bar{N}+M-1}\sum_{m=j'-\bar{N}+1}^{M} W_{pvm}C_{p(j'-m+1)p}(t,\ k,\ [\chi_{pq}+(j'-1)\tau_p]).$$

Consequently

$$\tilde{Z}^c_{pq}(t,\ \mathrm{v}) = \sum_{k=1}^{N_c}\left\{\overset{<}{R}{}^c_{pq}(t,\ \mathrm{v},\ k) + S^c_{pq}(t,\ \mathrm{v},\ k) + \overset{>}{R}{}^c_{pq}(t,\ \mathrm{v},\ k)\right\},$$

which is the rearrangement stated in the theorem.

Q.E.D

PROOF OF THE SEPARATION-TIME-INTERVAL THEOREM

In proving the separation-time-interval theorem, two cases arise, illustrated in Figs. 16 and 17.

Case 1: $\beta_k - \alpha_k > \tau_p$, Clutter Only

In case 1, if the leading edge of the first steady-state term given by the clutter separation signals $S^c_{pq}(t,\ \mathrm{v},\ k)$ given by

$$\alpha_k + \chi_{pq} + (M-1)\tau_p$$

is less than the beginning of kth-clutter-patch separation time interval

$$\text{integer}\left\{\frac{\beta_k + \chi_{pq}}{\tau_p}\right\}\tau_p + \tau_p + (M-2)\tau_p,$$

then the filter is in steady-state operation at the beginning of the kth-clutter-patch separation time interval. The result is

$$\alpha_k + (M-1)\tau_p + \chi_{pq} < \text{integer}\left\{\frac{\beta_k + \chi_{pq}}{\tau_p}\right\}\tau_p + (M-1)\tau_p.$$

Since $\beta_k > \tau_p + \alpha_k$, then

$$\frac{\alpha_k + \chi_{pq}}{\tau_p} < \text{integer}\left\{\frac{\tau_p + \alpha_k + \chi_{pq} + \text{additional time}}{\tau_p}\right\},$$

which is true.

In addition if the trailing edge of the last steady-state term given by the clutter separation signals $S^c_{pq}(t, v, k)$ given by

$$\beta_k + \chi_{pq} + (\bar{N} + M - 2)\tau_p$$

is greater than the right end of the kth-clutter-patch separation time interval

$$\text{integer}\left\{\frac{\alpha_k + \chi_{pq}}{\tau_p}\right\}\tau_p + \bar{N}\tau_p,$$

then the filter is in steady-state at the end of the kth-clutter-patch separation time interval. The result is

$$\beta_k + \chi_{pq} + (\bar{N} + M - 2)\tau_p > \text{integer}\left\{\frac{\alpha_k + \chi_{pq}}{\tau_p}\right\}\tau_p + \bar{N}\tau_p.$$

Since $\beta_k = \tau_p + \alpha_k + \epsilon$, then

$$(\alpha_k + \chi_{pq}) + \epsilon + (M-1)\tau_p > \text{integer}\left\{\frac{\alpha_k + \chi_{pq}}{\tau_p}\right\}\tau_p,$$

and since $M \geq 2$, then the result is true.

The two conditions imply that the filter was in steady-state operation (defined by separation signals) over the kth-clutter-patch separation time interval, since the steady-state terms defined by separation signal, extends over the entire kth-clutter-patch separation time interval and are covered by remainder signals on both ends.

Case 2: $\beta_k - \alpha_k < \tau_p$

We will prove that none of the separation signals (steady-state signals) are covered by the left and remainder signals. Then any separation signal which appears over the separation time interval is in steady state over this interval and is not covered by other signals.

If the leading edge of the separation signal $S^c_{pq}(t, v, k)$

$$\alpha_k + \chi_{pq} + (M-1)\tau_p$$

is greater than the trailing edge of the right remainder signal $\overset{>}{R}{}^c_{pq}(t, v, k)$

$$\beta_k + \chi_{pq} + (M-2)\tau_p,$$

then the first steady-state signal occurs after the last left remainder signal. The result is

$$\alpha_k + \chi_{pq} + (M-1)\tau_p > \beta_k + \chi_{pq} + (M-2)\tau_p,$$

or

$$\alpha_k + \tau_p > \beta_k,$$

or $\beta_k - \alpha_k < \tau_p$, which was the original condition.

If the trailing edge of the last steady-state term of $S^c_{pq}(t, \mathrm{v}, k)$

$$\beta_k + \chi_{pq} + (\bar{N}-1)\tau_p$$

is less than the end of the leading edge of the right remainder signals $\overset{>}{R}{}^c_{pq}(t, \mathrm{v}, k)$

$$\alpha_k + \chi_{pq} + \bar{N}\tau_p,$$

the last steady-state signal is not covered by the right remainder signals. The result is

$$(\bar{N}-1)\tau_p + \beta_k < \bar{N}\tau_p + \alpha_k,$$

or $\beta_k - \alpha_k < \tau_p$, which again was the original condition.

Q.E.D.

The target proofs are not given.

PROOF OF THE TIME-ALIGNMENT THEOREM

The proof of the time-alignment theorem is constructed for only targets, since the clutter case is analogous. We evaluate $\overset{<}{R}{}^T_{pq}(t, \mathrm{v}, l)$, $S^T_{pq}(t, \mathrm{v}, l)$, and $\overset{>}{R}{}^T_{pq}(t, \mathrm{v}, l)$ for $q = j'$ and obtain

$$\overset{<}{R}{}^T_{pq}(t, \mathrm{v}, l) = \sum_{q=1}^{M-1} \sum_{m=1}^{q} W_{pvm} T_{p(q-m+1)p}(t, l, [\bar{\zeta} + \lambda_N + (\bar{N}+M-2)\bar{\tau}]),$$

$$S^T_{pq}(t, \mathrm{v}, l) = \sum_{q=\bar{M}}^{\bar{N}} \sum_{m=1}^{M} W_{pvm} T_{p(q-m+1)p}(t, l, [\bar{\zeta} + \lambda_N + (\bar{N}+M-2)\bar{\tau}]),$$

$$\overset{>}{R}{}^T_{pq}(t, \mathrm{v}, l) = \sum_{q=\bar{N}+1}^{\bar{N}+m-1} \sum_{m=q-\bar{N}+1}^{M} W_{pvm} T_{p(q-m+1)p}(t, l, [\bar{\zeta} + \lambda_N + (\bar{N}+M-2)\bar{\tau}]).$$

We find for the lth target the filtered target echoes in the remainder and separation signals all occur at time $\lambda_{N_i} + (\bar{N}+M-2)\bar{\tau}$ for $q = j'$. This implies that there is at least one time when each filtered target echo from a single target given by $i = 1, 2, \ldots, N$ and $j' = 1, 2, \ldots, \bar{N}+M-1$ is present simultaneously in $\tilde{Z}_{pq}(t, \mathrm{v})$ for all values of $p = 1, 2, \ldots, N$ and $q = 1, 2, \ldots, \bar{N}+M-1$.

PROOF OF THE CONDITIONS ON ECLIPSING GIVEN IN TABLE 1

Referring to Fig. A1, we find the following relationships. First it takes $M-1$ pulses before the filter can reach steady-state operation. Added to this number is then the number of echoes being eclipsed that must pass through the filter before steady-state operation is reached using echoes not eclipsed. The steady-state condition exists until $\bar{N}$ echoes have been processed, and then the transient decay begins. Consequently the number of times the filter can obtain steady-state operation for a single target without using eclipsed or partially eclipsed echoes is given by $\bar{N} - (M-1) -$ number of echoes eclipsed. Since the number of echoes eclipsed is equal to $\bar{N} -$ the number of echoes not eclipsed, the desired result is obtained. If the result is negative, the result is not real and should be zero.

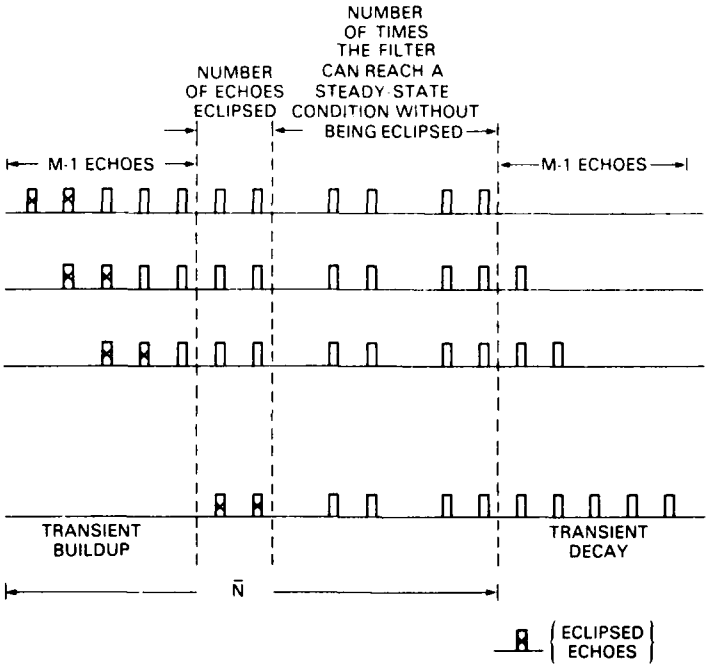

Fig. 1A — Counting used in determining eclipsing properties

Appendix B

PROOFS ON PULSE-DOPPLER AND MTI OPERATION

PROOF OF THE THEOREM ON THE NUMBER OF PULSES REQUIRED FOR PULSE-DOPPLER AND MTI OPERATION

Pulse-Doppler Operation

The left and right edges at the pulse-Doppler separation times for clutter are as follows. The left edge of $\bar{\Delta}_p^c$ is

$$\text{integer}\left\{\frac{\beta_{N_c}+\chi_{pq}}{\tau_p}\right\}\tau_p+\tau_p+(M-2)\tau_p,$$

and the right edge of $\bar{\Delta}_p^c$ is

$$\text{integer}\left\{\frac{\alpha_1+\chi_{pq}}{\tau_p}\right\}\tau_p+\bar{N}\,\tau_p.$$

The left and right edges of the pulse-Doppler separation times for targets are as follows. The left edge of $\bar{\Delta}_p^T$ is

$$\text{integer}\left\{\frac{\gamma_{N_T}+\chi_{pq}+\bar{\zeta}_i}{\tau_p}\right\}\tau_p+\tau_p+(M-2)\tau_p,$$

and the right edge of $\bar{\Delta}_p^T$ is

$$\text{integer}\left\{\frac{\gamma_1+\chi_{pq}-\bar{\zeta}_i}{\tau_p}\right\}\tau_p+\bar{N}\,\tau_p.$$

The greatest left edge caused by the requirement for $\bar{\Delta}_p^c \cap \bar{\Delta}_p^T$ is

$$\text{integer}\left[\max\begin{Bmatrix}(\beta_{N_c}+\chi_{pq})/\tau_p\\ \text{or}\\ (\gamma_{N_t}+\chi_{pq}+\bar{\zeta}_i)/\tau_p\end{Bmatrix}\right]\tau_p+(M-2)\tau_p+\tau_p.$$

The least right edge caused by the requirement for $\bar{\Delta}_p^c \cap \Delta_p^T$ is

$$\text{integer}\left[\min\begin{Bmatrix}(\alpha_1+\chi_{pq})/\tau_p\\ \text{or}\\ (\gamma_1+\chi_{pq}-\bar{\zeta}_i)/\tau_p\end{Bmatrix}\right]\tau_p+\bar{N}\,\tau_p.$$

The width of the time interval of $\bar{\Delta}_p^c \cap \bar{\Delta}_p^T$ is obtained by subtracting the left edge from the right edge, yielding

$$\text{integer}\left[\min\begin{Bmatrix}(\alpha_1+\chi_{pq})/\tau_p\\ \text{or}\\ (\gamma_1+\chi_{pq}-\bar{\zeta}_i)/\tau_p\end{Bmatrix}\right]\tau_p+\bar{N}\tau_p-\text{integer}\left[\max\begin{Bmatrix}(\beta_{N_c}+\chi_{pq})/\tau_p\\ \text{or}\\ (\gamma_{N_t}+\chi_{pq}+\bar{\zeta}_i)/\tau_p\end{Bmatrix}\right]\tau_p+(M-2)\tau_p.$$

This time interval must be greater than or equal to τ_p, where $p = i$, to meet the condition for pulse-Doppler operation. Invoking this condition and rearranging terms yields

$$\bar{N} \geqslant \text{integer}\left[\max\begin{Bmatrix}(\beta_{N_c} + \chi_{pq})/\tau_p \\ \text{or} \\ (\gamma_{N_t} + \chi_{pq} + \bar{\zeta}_i)/\tau_p\end{Bmatrix}\right] - \text{integer}\left[\min\begin{Bmatrix}(\alpha_1 + \chi_{pq})/\tau_p \\ \text{or} \\ (\gamma_1 + \chi_{pq} - \bar{\zeta}_i)/\tau_p\end{Bmatrix}\right] + M.$$

Q.E.D.

MTI Operation

For MTI operation

$$1 > \max\begin{Bmatrix}(\beta_{N_c} + \chi_{pq})/\tau_p \\ \text{or} \\ \gamma_{N_t} + \chi_{pq} + \bar{\zeta}_i)/\tau_p\end{Bmatrix} - \min\begin{Bmatrix}(\alpha_1 + \chi_{pq})/\tau_p \\ \text{or} \\ (\gamma_1 + \chi_{pq} - \bar{\zeta}_i)/\tau_p\end{Bmatrix}.$$

Consequently

$$\text{integer}\left[\max\begin{Bmatrix}(\beta_{N_c} + \chi_{pq})/\tau_p \\ \text{or} \\ (\gamma_{N_t} + \chi_{pq} + \bar{\zeta}_i)/\tau_p\end{Bmatrix}\right] - \text{integer}\left[\min\begin{Bmatrix}(\alpha_1 + \chi_{pq})/\tau_p \\ \text{or} \\ (\gamma_1 + \chi_{pq} - \bar{\zeta}_i)/\tau_p\end{Bmatrix}\right]$$

must be 0 or 1. Consequently

$$\bar{N} \geqslant M \text{ or } \bar{N} \geqslant M + 1.$$

Q.E.D.

PROOF OF THE PULSE-DOPPLER CLUTTER STACKING THEOREM

Pulse-Doppler Result

The clutter separation signal written as

$$S^c_{pq}(t, \mathrm{v}, k) = \sum_{j'=M}^{\bar{N}} \sum_{m=1}^{M} W_{p\mathrm{v}m}\, C_{p(j'-m+1)p}(t, k, [\bar{\zeta} + \lambda_N + (\bar{N} + M - 2)\bar{\tau} + (j' - 1)\tau_p - (q - 1)\tau_p])$$

is written in terms of the segmented clutter signals using the definition. The result is

$$S^c_{pq}(t, \mathrm{v}, k) = \sum_{u=1}^{N_k} \sum_{j'=M}^{\bar{N}} \sum_{m=1}^{M} W_{p\mathrm{v}m} \tilde{C}_{p(j'-m+1)p}\left(t, k, u, \left[\text{integer}\left\{\frac{\alpha_k + \chi_{pq}}{\tau_p}\right\}\tau_p + (j' - 1)\tau_p + (u - 1)\tau_p\right]\right),$$

where the order of summation has been changed. The sum over j' is broken into three parts, and the result is

$$\begin{aligned} S^c_{pq}(t, \mathrm{v}, k) = \sum_{u=1}^{N_k} \Bigg[& \sum_{j'=M}^{j'=M+N_k-u-1} \sum_{m=1}^{M} W_{p\mathrm{v}m} \tilde{C}_{p(j'-m+1)p}\left(t, k, u, \left[\text{integer}\left\{\frac{\alpha_k + \chi_{pq}}{\tau_p}\right\}\tau_p + (j' + u - 2)\tau_p\right]\right) \\ & + \sum_{j'=N_k-u+M}^{j'=\bar{N}-u+1} \sum_{m=1}^{M} W_{p\mathrm{v}m} \tilde{C}_{p(j'-m+1)p}\left(t, k, u, \left[\text{integer}\left\{\frac{\alpha_k + \chi_{pq}}{\tau_p}\right\}\tau_p + (j' + u - 2)\tau_p\right]\right) \\ & + \sum_{j'=\bar{N}-u+2}^{j'=\bar{N}} \sum_{m=1}^{M} W_{p\mathrm{v}m}\, \tilde{C}_{p(j'-m+1)p}\left(t, k, u, \left[\text{integer}\left\{\frac{\alpha_k + \chi_{pq}}{\tau_p}\right\} + (j' + u - 2)\tau_p\right]\right)\Bigg]. \end{aligned}$$

We rewrite the middle term (MT) of the sums defining $S^c_{pq}(t, v, k)$ as

$$\mathrm{MT} = \sum_{j'=N_k-u+M}^{j'=\bar{N}-u+1} \sum_{m=1}^{M} W_{pvm}\, \tilde{C}_{p(j'-m+1)p}\left(t,k,u,\left[\text{integer}\left\{\frac{\alpha_k + \chi_{pq}}{\tau_p}\right\}\tau_p + (j'-u-2)\tau_p\right]\right).$$

By defining

$$j'' = j' + u - 2,$$

we can rewrite the middle term as

$$\mathrm{MT} = \sum_{u=1}^{N_k} \sum_{j''=N_k+M-1}^{\bar{N}} \sum_{m=1}^{M} W_{pvm}\, \tilde{C}_{p(j''-m-u+1)p}\left(t,k,u,\left[\text{integer}\left\{\frac{\alpha_k + \chi_{pq}}{\tau_p}\right\}\tau_p + (j''-1)\tau_p\right]\right).$$

The order of summation can be reversed:

$$\mathrm{MT} = \sum_{j''=N_k+M-1}^{\bar{N}} < \sum_{u=1}^{N_k}\left\{\sum_{m=1}^{M} W_{pvm}\, \tilde{C}_{p(j''-m-u+1)p}\left(t,k,u,\left[\text{integer}\left\{\frac{\alpha_k + \chi_{pq}}{\tau_p}\right\}\tau_p + (j''-1)\tau_p\right]\right)\right\} > .$$

The terms in the angular brackets all appear at the same time. The inner sum, in braces, is the steady-state filtered signals due to the echoes from the uth clutter segment. The middle sum is over all clutter segments. Consequently the steady-state filtered signals are due to echoes from all clutter segments $u = 1, 2, \ldots, N_k$ at any instant of time.

The next part we have to prove is that the terms in MT extend over the pulse-Doppler separation time interval. The leading edge of the first term of MT occurs at time

$$\text{integer}\left\{\frac{\alpha_k + \chi_{pq}}{\tau_p}\right\}\tau_p + (N_k + M - 2)\tau_p$$

and must be less than or equal to the left edge of the pulse-Doppler separation time interval given by

$$\chi_{pq} + (M-2)\tau_p + \beta_k.$$

Consequently

$$\text{integer}\left\{\frac{\alpha_k + \chi_{pq}}{\tau_p}\right\}\tau_p + (N_k + M - 2)\tau_p \leqslant (M-2)\tau_p + \beta_k + \chi_{pq},$$

which can be rewritten as

$$N_k \leqslant (\beta_k + \chi_{pq}) - \text{integer}\left\{\frac{\alpha_k + \chi_{pq}}{\tau_p}\right\}.$$

By definition

$$N_k = \text{integer}\left\{\frac{\beta_k + \chi_{pq}}{\tau_p}\right\} - \text{integer}\left\{\frac{\alpha_k + \chi_{pq}}{\tau_p}\right\} + 1.$$

Combining yields the desired result:

$$\text{integer}\left\{\frac{\beta_k + \chi_{pq}}{\tau_p}\right\} + 1 \leqslant (\beta_k + \chi_{pq}).$$

The trailing edge of the last term in MT occurs at the time

$$\text{integer}\left\{\frac{\alpha_k + \chi_{pq}}{\tau_p}\right\}\tau_p + (\bar{N} - 1)\tau_p + \tau_p$$

and must be greater than or equal to the right edge of the pulse-Doppler separation time interval given by

$$\text{integer}\left\{\frac{\alpha_k + \chi_{pq}}{\tau_p}\right\}\tau_p + \bar{N}\,\tau_p.$$

Consequently the MT terms extend over the pulse-Doppler separation time interval.

By the definitions of pulse-Doppler operation, the separation signal $S^c_{pq}(t, \mathrm{v}, k)$ is composed of clutter echoes from all clutter patches over the pulse-Doppler separation time interval for clutter on the pth pulse train. Consequently from the previous part of the proof on clutter segments we conclude the following. The signal $S^c_{pq}(t, \mathrm{v}, k)$ is composed of all clutter segments of all clutter patches at any instant of time under the pulse-Doppler conditions.

Q.E.D.

Result When the MTI Condition is Met

If the MTI condition is met, N_k is either equal to 1 or 2. If N_k equals 1, which is the case illustrated by Fig. B1, then the previous pulse Doppler result for MT applies and is written as

$$\mathrm{MT} = \sum_{j''=N_k+M-1}^{\bar{N}} \sum_{M=1}^{N_k-1}\left\{\sum_{m=1}^{M} W_{pvm}\,\tilde{C}_{p(j''-m-u+1)p}\left(t,k,u,\left[\text{integer}\left\{\frac{\alpha_k + \chi_{pq}}{\tau_{pq}}\right\}\tau_p + (j''-1)\tau_p\right]\right)\right\}.$$

Since there is only one clutter segment term, there is only clutter segment at any instant of time for the kth clutter patch. Furthermore because clutter patches are disjoint, that is,

$$\alpha_1 < \beta_1 < \alpha_2 < \beta_2 < \alpha_3 < \beta_3 < \ \ldots < \alpha_{N_c} < \beta_{N_c},$$

and the MTI conditions are met, the terms due to all clutter patches are disjoint. Consequently the separation signal $S^c_{pq}(t, \mathrm{v}, k)$ is composed of only one clutter segment from one clutter patch at any instant in time.

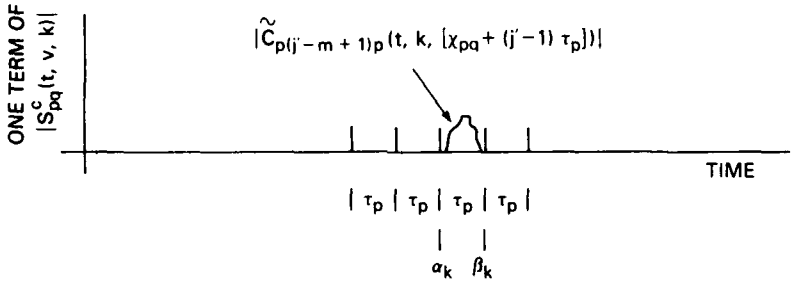

Fig. B1 — Location of the clutter echo $N_k = 1$

If N_k equals 2 which is the case illustrated by Fig. B2, then for $u = 1$ and $u = 2$ the clutter segments occupy different intervals of time as long as the MTI conditions are met. Consequently the clutter segments are disjoint in time. Furthermore, because clutter patches are disjoint and the MTI conditions are met, the terms due to all clutter patches are disjoint. Consequently the separation signal $S^c_{pq}(t, \mathrm{v}, k)$ is composed of only one clutter segment from one clutter patch at any instant of time.

Q.E.D.

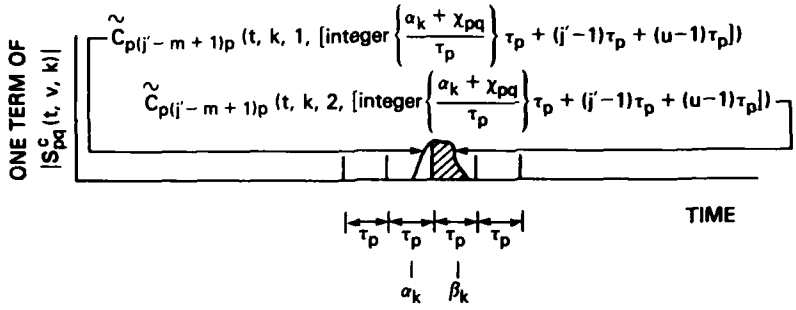

Fig. B2 — Location of the clutter echo $N_k = 2$

PROOF OF THE COUNTING THEOREM

From the proof of the theorem on the number of pulses required for pulse-Doppler and MTI operation we found the right edge minus the left edge of the pulse-Doppler separation time interval to be

$$\text{integer}\left[\min\begin{Bmatrix}(\alpha_1 + \chi_{pq})/\tau_p \\ \text{or} \\ (\gamma_1 + \chi_{pq} - \bar{\zeta}_i)/\tau_p\end{Bmatrix}\right]\tau_p + \bar{N}\tau_p - \text{integer}\left[\max\begin{Bmatrix}(\beta_{N_c} + \chi_{pq})/\tau_p \\ \text{or} \\ (\gamma_{N_t} + \chi_{pq} + \bar{\zeta}_i)/\tau_p\end{Bmatrix}\right]\tau_p + (M-2)\tau_p.$$

This quantity is equal to $N_s\tau_p$, which is the time interval in which N_s target separation signals can occur. We recall that target separation signals occur clear across the pulse-Doppler separation time interval for pulse-Doppler operation. Consequently the terms can be arranged to give the result

$$N_s = \text{integer}\left[\min\begin{Bmatrix}(\alpha_1 + \chi_{pq})/\tau_p \\ \text{or} \\ (\gamma_1 + \chi_{pq} - \bar{\zeta}_i)/\tau_p\end{Bmatrix}\right] - \text{integer}\left[\max\begin{Bmatrix}(\beta_{N_c} + \chi_{pq})/\tau_p \\ \text{or} \\ (\gamma_1 + \chi_{pq} + \bar{\zeta}_i)/\tau_p\end{Bmatrix}\right] + (\bar{N} - M + 1).$$

Q.E.D.

Appendix C

PROOFS ON CONTROLLED-PULSE-DOPPLER (CPD) OPERATION

PROOF OF THE THEOREM ON THE NUMBER OF PULSES REQUIRED FOR CPD OPERATION

The left and right edge of the pulse-Doppler separation times for the kth clutter patch on the pth pulse train are as follows. The left edge of Δ_{kp}^{c} is

$$\text{integer}\,\{(\beta_k + \chi_{pq})/\tau_p\}\,\tau_p + \tau_p + (M-2)\tau_p,$$

and the right edge of Δ_{kp}^{c} is

$$\text{integer}\,\{(\alpha_k + \chi_{pq})/\tau_p\}\,\tau_p + \bar{N}\tau_p.$$

The right edge must exceed the left edge by one pulse-repetition interval, which yields

$$\text{integer}\,\{(\alpha_k + \chi_{pq})/\tau_p\}\,\tau_p + \bar{N}\,\tau_p \geqslant \text{integer}\,\{(\beta_k + \chi_{pq})/\tau_p\}\,\tau_p + \tau_p + \tau_p + (M-2)\tau_p.$$

Solving for $\bar{N}$ yields

$$\bar{N} \geqslant \text{integer}\,\{(\beta_k + \chi_{pq})/\tau_p\} - \text{integer}\,\{(\alpha_k + \chi_{pq})/\tau_p\} + M.$$

For MTI operation $\beta_k - \alpha_k < \tau_p$. Then

$$\text{integer}\,\{(\beta_k + \chi_{pq})/\tau_p\} - \text{integer}\,\{(\alpha_k + \chi_{pq})/\tau_p\}$$

may be either 0 or 1, and consequently

$$\bar{N} \geqslant M \text{ or } \bar{N} \geqslant M+1.$$

Q.E.D.

PROOF OF THE CPD COUNTING THEOREM

From the proof of the theorem on the number of pulses required for CPD operation we found the right edge minus the left edge of the separation time interval Δ_{kp}^{c} to be

$$\text{integer}\,\{(\alpha_k + \chi_{pq})/\tau_p\}\,\tau_p + \bar{N}\,\tau_p - \{\text{integer}\,\{(\beta_k + \chi_{pq})/\tau_p\}\,\tau_p + \tau_p + (M-2)\tau_p\}.$$

This quantity is equal to $N_s(k)\tau_p$, which is the time interval in which $N_s(k)$ target separation signals can occur. Consequently the terms can be rearranged to yield

$$N_s(k) = \text{integer}\,\{(\alpha_k + \chi_{pq})/\tau_p\} - \text{integer}\,\{(\beta_k + \chi_{pq})/\tau_p\} + (\bar{N} - m + 1).$$

PROOF OF THE THEOREM ON CPD SEPARATION REQUIREMENT 1

The left edge of $\overset{<}{R}{}_{pq}^{c}(t, \text{v}, k+1)$ must occur after the right edge of Δ_{kp}^{c}. This is written as

$$\alpha_{k+1} + \chi_{pq} \geqslant \text{integer}\,\{(\alpha_k + \chi_{pq})/\tau_p\}\,\tau_p + \bar{N}\,\tau_p.$$

We note the previous result

$$N_s(k) = \text{integer}\,\{(\alpha_k + \chi_{pq})/\tau_p\} - \text{integer}\,\{(\beta_k + \chi_{pq})/\tau_p\} + (\bar{N} - M + 1).$$

Combining these two equations yields the result

$$\alpha_{k+1} \geqslant \text{integer}\,\{(\beta_k + \chi_{pq})/\tau_p\}\tau_p - \chi_{pq} + (N_s(k) + M - 1)\,\tau_p.$$

Furthermore the left edge of Δ^{ℓ}_{kp} must exceed the right edge of $\overset{<}{R}{}^{c}_{pq}$ $(t, v, k-1)$. This is written as

$$\text{integer}\,\{(\beta_k + \chi_{pq})/\tau_p\}\,\tau_p + \tau_p + (M-2)\tau_p \geqslant \beta_{k-1} + \chi_{pq} + (\bar{N} + M - 2)\tau_p.$$

Combining this equation with the requirement for N_S, we obtain

$$\text{integer}\,\{(\alpha_k + \chi_{pq})/\tau_p\} - \chi_{pq} \geqslant \beta_{k-1} + (N_s(k) + M - 2)\,\tau_p.$$

Q.E.D.

PROOF OF THE THEOREM ON CPD SEPARATION REQUIREMENT 2

The trailing edge of the $(k-1)$th right remainder signal must not cover the separation time interval from $s\,\tau_p$ to $(s+1)\tau_p$ from its left edge. As shown in Fig. 24, this requires

$$\text{integer}\,\{(\alpha_k + \chi_{pq})/\tau_p\}\,\tau_p + \bar{N}\,\tau_p - (N_s(k) - s)\tau_p \geqslant \beta_{k-1} + \chi_{pq} + (\bar{N} + M - 2)\tau_p.$$

Furthermore the leading edge of the $(k+1)$th left remainder signal must not cover the separation time interval from $s\,\tau_p$ to $(s+1)\tau_p$ from its left edge. From Fig. 24, this requires

$$\alpha_{k+1} + \chi_{pq} \geqslant \text{integer}\,[(\beta_k + \chi_{pq})/\tau_p]\tau_p + \tau_p + (M-2)\tau_p + (s+1)\tau_p.$$

The proof is completed by noting that since the range extent of the k^*th patch is longer than that of the kth patch, the separation time interval is sufficient for the kth patch if it is not covered by the $(k-1)$th or $(k+1)$th patch signals.

Q.E.D.

PROOF OF THE THEOREM ON TARGET RANGE AMBIGUITIES FOR CPD OPERATION

The last target echo after passing through the filter of the γth target is located at a time

$$\gamma_l + \chi_{pq} + (\bar{N} + M - 2)\tau_p,$$

which must be greater than the trailing edge of the separation time interval Δ^{ℓ}_{kp}, yielding

$$\gamma_l + \chi_{pq} + (\bar{N} + M - 2)\,\tau_p > \text{integer}\,\{(\alpha_k + \chi_{pq})/\tau_p\}\,\tau_p + \bar{N}\,\tau_p.$$

Rearranging terms yields

$$\gamma_l > \text{integer}\,\{(\alpha_k + \chi_{pq})/\tau_p\}\,\tau_p - \chi_{pq} - (M-2)\tau_p.$$

Furthermore the first target echo after passing through the filter of the γth target is located at a time

$$\gamma_l + \chi_{pq},$$

which must be less than the leading edge of the separation time interval Δ^{ℓ}_{kp}, yielding

$$\gamma_l + \chi_{pq} < \text{integer}\,\{(\beta_k + \chi_{pq})/\tau_p\}\,\tau_p + \tau_p + (M-2)\tau_p.$$

Rearranging terms yields

$$\gamma_l < \text{integer}\,\{(\beta_k + \chi_{pq})/\tau_p\}\,\tau_p - \chi_{pq} + (M-1)\tau_p.$$

The number of range ambiguities is obtained by subtracting $\gamma_l^{\max} - \gamma_l^{\min}$ and dividing by τ_p, yielding

$$(\gamma_l^{\max} - \gamma_l^{\min})/\tau_p = \text{integer}\,\{(\beta_k + \chi_{pq})/\tau_p\} - \text{integer}\,\{(\alpha_k + \chi_{pq})/\tau_p\} + 2M - 3.$$

Q.E.D.

END

FILMED

6-83

DTIC